Biomedicine & Pharmacotherapy 142 (2021) 112019

Contents lists available at ScienceDirect

Biomedicine & Pharmacotherapy

journal homepage: www.elsevier.com/locate/biopha

Impaired brown adipose tissue is differentially modulated in insulin-resistant obese wistar and type 2 diabetic Goto-Kakizaki rats

Tamires Duarte Afonso Serdan [a,*], Laureane Nunes Masi [a], Joice Naiara Bertaglia Pereira [a], Luiz Eduardo Rodrigues [a], Amanda Lins Alecrim [a], Maria Vitoria Martins Scervino [a], Vinicius Leonardo Sousa Diniz [a], Alef Aragão Carneiro dos Santos [a], Celso Pereira Batista Sousa Filho [a], Tatiana Carolina Alba- Loureiro [a], Gabriel Nasri Marzuca-Nassr [b], Roberto Barbosa Bazotte [c], Renata Gorjão [a], Tania Cristina Pithon-Curi [a], Rui Curi [a], Sandro Massao Hirabara [a]

[a] Interdisciplinary Postgraduate Program in Health Sciences, Cruzeiro do Sul University, São Paulo, Brazil
[b] Department of Internal Medicine, Faculty of Medicine, Universidad de La Frontera, Temuco, Chile
[c] Department of Pharmacology and Therapeutics, State University of Maringa, Paraná, Brazil

ARTICLE INFO

Keywords:
Obesity
Type 2 diabetes
Thermogenesis
Batokines
Glucose uptake

ABSTRACT

Brown adipose tissue (BAT) is a potential target to treat obesity and diabetes, dissipating energy as heat. Type 2 diabetes (T2D) has been associated with obesogenic diets; however, T2D was also reported in lean individuals to be associated with genetic factors. We aimed to investigate the differences between obese and lean models of insulin resistance (IR) and elucidate the mechanism associated with BAT metabolism and dysfunction in different IR animal models: a genetic model (lean GK rats) and obese models (diet-induced obese Wistar rats) at 8 weeks of age fed a high-carbohydrate (HC), high-fat (HF) diet, or high-fat and high-sugar (HFHS) diet for 8 weeks. At 15 weeks of age, BAT glucose uptake was evaluated by 18F-FDG PET under basal (saline administration) or stimulated condition (CL316,243, a selective β3-AR agonist). After CL316, 243 administrations, GK animals showed decreased glucose uptake compared to HC animals. At 16 weeks of age, the animals were euthanized, and the interscapular BAT was dissected for analysis. Histological analyses showed lower cell density in GK rats and higher adipocyte area compared to all groups, followed by HFHS and HF compared to HC. HFHS showed a decreased batokine FGF21 protein level compared to all groups. However, GK animals showed increased expression of genes involved in fatty acid oxidation (CPT1 and CPT2), BAT metabolism (Sirt1 and Pgc1-α), and obesogenic genes (leptin and PAI-1) but decreased gene expression of glucose transporter 1 (GLUT-1) compared to other groups. Our data suggest impaired BAT function in obese Wistar and GK rats, with evidence of a whitening process in these animals

1. Introduction

Obesity is considered a public health problem that is characterized by an imbalance in energy intake and energy expenditure; obesity has been directly associated with type 2 diabetes (T2D), which is characterized by insulin resistance (IR) in adipose tissue, skeletal muscle, and liver [1,2] and could be related to lifestyle or genetic factors [3]. In addition, although it is well known that obesogenic diets lead to a body weight increase and IR, few studies have shown the intensity levels related to the effect of the main macronutrient diet composition or the association of both macronutrients, such as fat and sugar [3–5]. Nevertheless, T2D is conventionally attributed to obesity, mainly in the Western world population; however, in the Asian population, 70% of T2D patients are lean (BMI < 25) [6–8]. Thus, understanding the mechanisms involved in IR in obese and lean models is essential; furthermore, over the last decades, several researchers have been studying options to treat obesity and T2D.

Brown adipose tissue (BAT) is required for nonshivering thermoregulation, presenting a high thermogenesis capacity, regulating systemic metabolism, participating in glycemic homeostasis, and

* Correspondence to: Rua Galvao Bueno, 868, Liberdade, São Paulo, SP 01506-000, Brazil.
E-mail address: tamiresd.serdan@gmail.com (T.D.A. Serdan).

https://doi.org/10.1016/j.biopha.2021.112019
Received 12 May 2021; Received in revised form 29 July 2021; Accepted 7 August 2021
Available online 14 August 2021

displaying high metabolic activity due to the presence of uncoupling protein-1 (UCP1). Due to the ability to dissipate energy, that is, to oxidize excess food metabolites, BAT has been proposed as a potential target for obesity treatment [9]. In addition, several factors modulate BAT function. Its activity is regulated by adrenergic receptors and the sympathetic nervous system (SNS); different signals can lead to recruitment or atrophy of BAT. Its thermogenic capacity is regulated by cold exposure or by β3-adrenergic receptor (Adrb3) signaling activation [10]. Norepinephrine (NE) is the effector of acute thermogenesis, acting via adrenergic receptors. Furthermore, studies have shown that BAT is involved in regulating systemic metabolism because of its high energetic expenditure [11,12].

Despite those features, several factors can reduce BAT function, which could be linked mainly to metabolic dysfunction. In contrast, although BAT presents low susceptibility to the development of inflammation, the induction of proinflammatory cytokines can occur due to obesity and IR [13,14]. Induction of proinflammatory cytokines has been associated with impaired BAT function, such as IR, impaired glucose uptake, and SNS activity, resulting in NE release impairment and hence impaired thermogenic response. Few studies have focused on the impact of molecular mechanisms, such as IR, which may contribute to BAT dysfunction, a process named “whitening” [15–17]. However, how this BAT dysfunction occurred in response to IR remains to be elucidated.

Different rat models have been used to investigate the insulin resistance mechanisms aiming to translate to human disorders. Herein, we used models of obese rats induced by obesogenic diets (classic models in the literature to study IR induced by obesity), and GK rats, a genetic model of insulin resistance, which is used as a model to investigate the complications related to T2DM without obesity, to analyze the effect of these insulin resistance models on BAT function. This model was developed through selective breeding of glucose-intolerant Wistar rats [18,19]. These animals develop T2D earlier in their life, when 28 days old presents hyperglycemia, IR, impaired insulin secretion by pancreatic β-cells, increased plasma triglycerides, liver glucotoxicity, and liver inflammation [1]; curiously, the same changes were also reported in high-fat (HF) diet-induced obesity. These animals have been largely used to investigate the development of T2D without obesity and its consequences on physiological systems. Interestingly, similar to rats subjected to obesogenic diets, GK rats display impaired insulin sensitivity and T2D [1,20,21]. In this study, we aimed to elucidate the mechanism associated with BAT metabolism and dysfunction in different IR animal models: a genetic model (GK rats) and diet-induced obesity models, including a high-fat diet (HF) and a high-fat and high-sugar diet (HFHS). We expect that our findings could help other research groups understand the effect of different IR models on impaired BAT function.

2. Materials and methods

2.1. Ethics approval

The animal studies were performed according to protocols approved by the Committee on Ethics in the Use of Animals (CEUA) of Cruzeiro do Sul University (number 024/2017). All experiments were performed in accordance with relevant guidelines and regulations.

2.2. Animals

Male adult Wistar and Goto-Kakizaki rats were obtained from Charles River Laboratories International Inc. (Wilmington, MA, USA) and maintained at the animal facility of the Interdisciplinary Postgraduate Program in Health Sciences, Cruzeiro do Sul University. The rats were housed in a room with a light-dark cycle of 12–12 h, constant temperature at 23 ± 2 °C, circulating air, and free access to water and food (standard rodent diet, Nuvilab CR-1, Quimtia, S/A, Colombo, PR, Brazil) until 8 weeks of age.

2.3. Experimental protocol

At 8 weeks of age, a total of 65 animals, divided into the four groups, was used in this study. The following groups were investigated: (1) Wistar fed a high-carbohydrate diet (HC) (energy composition of 70% carbohydrate, 20% protein and 10% fat; 3,85 kcal/g; Rhoster, São Paulo, Brazil); (2) Wistar fed a high-fat diet (HF) (energy composition of 60% fat, 20% protein and 20% carbohydrate; 5,24 kcal/g; Rhoster, São Paulo, Brazil); (3) Wistar fed a high-fat and high-sugar (HFHS) (condensed milk, energy composition of 68% carbohydrate, 23% fat and 9% protein; 3,25 kcal/g, Glória, São Paulo, Brazil), and (4) GK group fed an HC (GK). All diets and water were administered ad libitum for 8 weeks. Diets were obtained from Rhoster Company (Araçoiaba da Serra, SP, Brazil), and their composition was established based on Research Diets, Inc. (New Brunswick, NJ, USA): D12450B (HC) and D12492 (HF). Body mass, food intake, and energy consumption were weekly assessed by a precision scale (Mettler Toledo PB001, Barueri, SP, Brazil). At 15 weeks of age, the GTT and ITT were performed. At 16 weeks of age, the animals were euthanized and the interscapular BAT was dissected for protein extraction, RNA extraction, and histological analyzes on the same animals. After euthanasia, the interscapular BAT was dissected, weighted, and stored at −80 °C for further analyses. Different adipose tissue deposits (retroperitoneal, epididymal, mesenteric, and inguinal) were removed and weighted.

2.4. Glucose tolerance test (GTT)

At 15 weeks of age, GTT was evaluated after 12 h of fasting. First, animals were intraperitoneally injected (i.p.) with a 50% glucose solution (2 g/kg body weight). Blood samples were obtained from a tail tip cut, and blood glucose measurements were performed at 0, 15, 30, 60, 90, and 120 min after injection. The concentration was determined using a blood glucose monitor (AccuCheck, Roche, SP, Brazil). The glucose concentration versus time was plotted, and the area under the curve (AUC) was calculated for each animal [1,22].

2.5. Insulin tolerance test (ITT)

Two days later, GTT and ITT were evaluated after 12 h of fasting. Initially, animals were injected i.p. with insulin (Humulin R; Lilly, Indianapolis, USA) using a dose of 0.5 IU/kg body weight. Blood samples were obtained from a tail tip cut, and blood glucose measurements were performed at 0, 4, 8, 12, 15, 20, and 30 min after injection. The rate constant for the ITT (kITT) was calculated based on the linear decline of blood glucose concentrations obtained from 0 to 30 min of the ITT curve [23,24]. The glucose concentration versus time was plotted, and the area under the curve (AUC) was calculated for each animal.

2.6. Animal experimental procedure

The PET study was performed at 14 weeks of age, after 6 weeks of diet administration. At this age, these animals displayed well-established increased body weight and insulin resistance. For this experimental protocol, the animals were moved to another animal facility, where it should be transported with enable time to reduce stress before the analysis. At the end of the experimental protocol, the animals were returned to the animal facility at Cruzeiro do Sul University with enable time of stress reduction before the animal euthanasia.

2.7. Determination of insulin and leptin concentration

At 16 weeks of age, after 12 h fasting, quantification of insulin and leptin in serum was performed using the enzyme-linked immunosorbent assay (ELISA) kit. The following kits commercially available from

Table 1
Sequence of primers used in the present study.

Gene	Forward sequence	Reverse sequence	Access number
IRS1	CCTCACCAACCCTTAGGCAG	GTCTTTCATTCTGCCTGTGACG	NM_012969.2
IRS2	GCCACCGTGGTGAAAGAGTA	AGCGTTGGTTGGAAACATGC	NM_001168633.1
PAI-1	CGTCTTCCTCCACAGCCATT	GTTGGATTGTGCCGAACCAC	M24067.1
Citrate synthase	CGGTTCTTGATCCTGATGAGGG	ACTGTTGAGGGCTGTGATGGC	XM_032909031.1
GPx-1	CCGGGACTACACCGAAATGA	TGCCATTCTCCTGATGTCCG	NM_030826.4
MAPK3	TCAGGACCTCATGGAGACGGAC	AGCCAGAATGCAGCCCACAG	NM_017347.3
GLUT1	GCTGTACGGCAAGATCGCTGAG	TTCAATCATGTCACCCACGCTG	AF032120.1
GLUT4	GCTGTGCCATCTTGATGACGG	TGAAGAAGCCAAGCAGGAGGAC	KT377191.1
Pgc1-α	CCCATACACAACCGCAGTCG	CTTCCTTTCCTCGTGTCCTCG	NM_031347.1
GSK 3β	ATCCTTATCCCTCCTCACGCTC	GACCAGTGTTGCTGAGTGGCAC	NM_032080.1
FASN	TGGTGAAGCCCAGAGGGATC	CACTTCCACACCCATGAGCG	NM_017332.2
CPT1	ATTCCAGGAGAGTGCCAGGAGG	CCCATGTCCTTGTAATGTGCGAG	NM_031559.2
CPT2	CACAACATCCTGTCCACCAGCAC	GAAACTCTCGGGCATTGCGTC	XM_032900786.1
FGF21	AACTCTCTATGGATCGCCTCAC	ACTCCTGGTTGCTCTTGGG	NM_130752.1
Cidea	TGTTAAGGAGTCTGCTGCGG	GGATGGCTGCTCTTCTGTGT	NM_001170467.1
Sirt1	TGTTTCCTGTGGGATACCTGA	TGAAGAATGGTCTTGGGTCTTT	NM_001372090.1
Leptin	AGCAGCTGCAAGGTCCAAG	TCCAGCACATTTTCCTCGCT	NM_013076.3
Adiponectin	GGTCACAATGGGATACCGGG	GACCAAGAACACCTGCGTCT	NM_144744.3
Resistin	TGTGTCCCATGGATGAAGCC	TCATTGCAGCTGGCAGTAGG	NM_144741.1
UCP-1	GCCTCTACGATACGGTCCAA	TGCATTCTGACCTTCACCAC	NM_012682.2
PPARα	ACGATGCTGTCCTCCTTGATG	GCGTCTGACTCGGTCTTCTTG	NM_013196.2
PPARγ	CCCTTTACCACGGTTGATTTCTC	GCAGGCTCTACTTTGATC GCACT	NM_013124.3
Adrb3	CGCACCTTGGGTCTCATTAT	GAAGGCAGAGTTGGCATAGC	NM_013108.2
GAPDH	TACAGCAACAGGGTGGTGGACC	TGGGATGGAATTGTGAGGGAGAG	XM_040978786.1

Sigma-Aldrich were used to determine serum levels of insulin (Ins1/ insulin ELISA kit #RAB0904-1KT), and leptin (Rat leptin ELISA kit #RAB0335-1KT). All the used kits according to the manufacturer's instruction. The absorbances were read using Fluostar Omega Spectrofluorimeter (FLUOstar Omega; BMG LABTECH, Ortenberg, Germany). The homeostatic model assessment – Insulin Resistance (HOMA-IR) index was calculated by the following formula: HOMA-IR = [glycemia (mM) × insulin (mU/L)]/ 22.5. The homeostatic model assessment – Beta (HOMA-B) index was calculated by the following formula: HOMA-B = 20 × Insulin (mU/L)÷ (glycemia (mM) - 3,5) [25]. In addition, the quantitative insulin sensitivity check (QUICKI) index was calculated by the following formula: QUICKI = 1/ (log basal glycemia + log basal insulin) [26].

2.8. RT-PCR gene expression measurements

Approximately 20 mg of BAT was pulverized in liquid nitrogen. Total RNA from BAT was extracted using TRIzol reagent (Invitrogen Life Technologies, Carlsbad, CA, USA). The concentration and purity (A260/280 and A260/230 ratio) were measured on a NanoDrop 2000 (Thermo Fisher Scientific, Uniscience, São Paulo, Brazil). cDNA was synthesized from 2 μg of total RNA by reverse transcription carried out with the High Capacity cDNA Reverse Transcription Kit (Applied Biosystems, Foster City, CA, USA). The mRNA expression levels of brown adipocyte genes, glucose metabolism and the insulin pathway were evaluated by real-time qPCR (polymerase chain reaction) using a *Quant Studio 3 Real-time PCR system* (Thermo Fisher Scientific, Waltham, MA, USA) and SYBR green (Platinum SYBR Green qPCR Supermix UDG, Invitrogen, CA, USA) as fluorescent dyes. The reference genes were defined in preliminary assays that indicated unaffected expression levels under the experimental conditions used herein. Gene expression was analyzed by the $2^{-\Delta\Delta CT}$ method using GAPDH as a reference gene. The primer sequences used in the present study are described in Table 1.

2.9. Western blot analysis

For protein measurements, interscapular BAT was dissected, weighed, and stored at −80 °C. Tissue was homogenized in RIPA buffer containing protease inhibitor cocktail (Complete-Mini, Roche). Protein content was determined in the supernatant of tissue extract using a BCA kit (Thermo Scientific, Rockford, IL, USA), and 5× Laemmli Sample Buffer was added to the samples. An equal amount of protein (30 μg) was separated by SDS-PAGE 10% polyacrylamide gel electrophoresis (acrylamide/bis-acrylamide = 37.5/1) and transferred to nitrocellulose membranes using a semidry electrophoretic transfer machine (Transblot Turbo, Bio-Rad). After being washed, the membranes were blocked in 5% milk for 1 h at room temperature and incubated with the indicated specific primary antibodies overnight at 4 °C. Then, the cells were incubated with secondary antibody conjugated to horseradish peroxidase, and the immunoblots were visualized with enhanced chemiluminescence (ECL kit; GE Healthcare Life Sciences) in a charge-coupled device camera (Amersham Biosciences). The relative band intensity was measured using Fiji/ImageJ software, and Ponceau staining was used as an internal control [1] UCP1 polyclonal antibody (1:1000, ab10983) and FGF21 polyclonal antibody (1:1000; ab171941) were purchased from Abcam (Abcam, Cambridge, UK). The antibody information used in the present study are described in Table 2.

Table 2
Antibody used in the present study.

Polyclonal antibody	Dilution factor	Catalog number	Molecular weight
UCP1	1:1000	ab10983	34 kDa
FGF21	1:1000	ab171941	22 kDa

2.10. Positron emission tomography with 2-deoxy-2-[fluorine-18]fluoro-D-glucose integrated with computed tomography (^{18}F-FDG PET/CT)

To evaluate BAT activity, ^{18}F-FDG PET/CT analysis was performed at 14 weeks of age, after 6 weeks of diet administration, using a small-animal PET/CT Scanner (Inveon; Siemens) without respiratory gating. At this age, these animals displayed well-established increased body weight and IR. Briefly, animals were housed 24 h before the PET/CT scan analysis at the facility of the Nuclear Medicine Laboratory (LIM-43), University of São Paulo, São Paulo, Brazil. The bolus of 141.5 MBq 18F-FDG was administered under basal condition or adrenergic stimulation. Under stimulated conditions, an intravenous injection of CL316,243 (1 mg/kg) was given 30 min before 18F-FDG treatment. In the basal state, animals received an intravenous saline injection. Imaging was performed one hour later under isoflurane inhalation anesthesia (1.5%). Room temperature was strictly maintained between 23 and

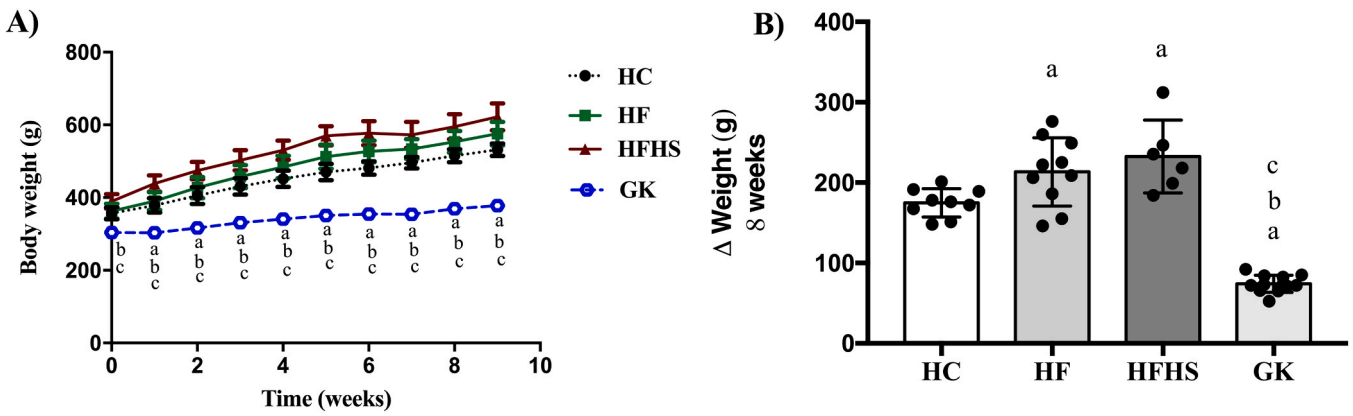

Fig. 1. Body weight evaluation (A) and body weight gain (B) after 8 weeks of diet. HC = Wistar fed a high-carbohydrate diet (n = 8); HF = Wistar fed a high-fat diet (n = 8); HFHS = Wistar fed a high-fat high-sugar diet (n = 6); GK = Goto-Kakizaki fed a high-carbohydrate diet (n = 10). The results are expressed as the mean ± S. D. (a) $p < 0.05$ compared with HC; (b) $p < 0.05$ compared with HF; (c) $p < 0.05$ compared with HFHS, using one-way ANOVA and Tukey's posttest.

25 °C. Polygonal regions of interest were drawn on sagittal PET/CT slices for interscapular BAT. Circular regions of interest were placed in the left lung as background activity. From each region of interest, mean standardized uptake values (SUVs mean) and target-to-background ratios were measured as indices of ^{18}F-FDG uptake.

2.11. Histological preparation of the tissue samples

After 16 weeks of the experimental period, animals were euthanized as previously described, and depots of interscapular BAT were dissected and freshly fixed in 4% paraformaldehyde-phosphate-buffered for 72 h.

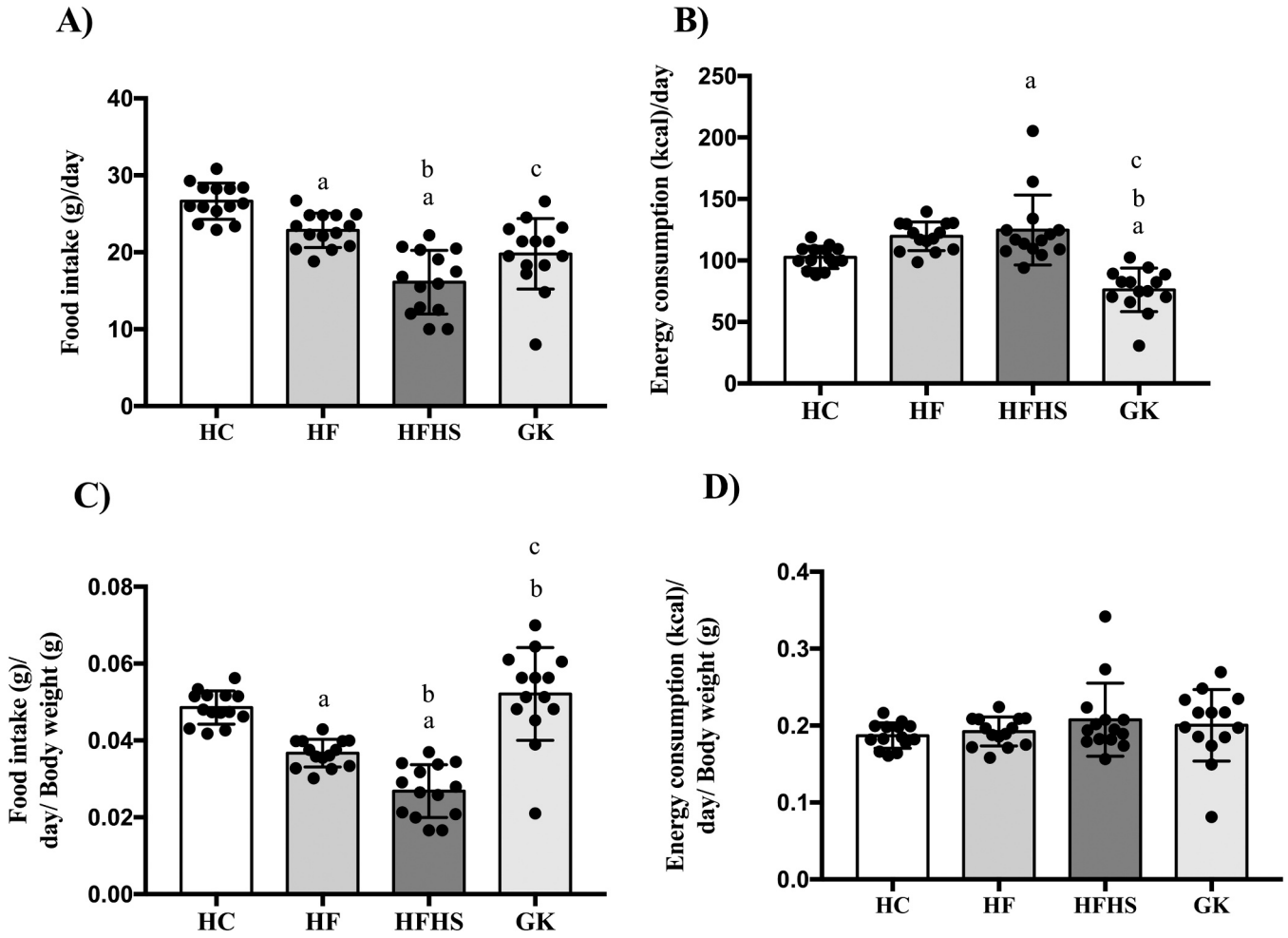

Fig. 2. Food intake (g)/day (A) Energy consumption (kcal)/day (B) Food intake (g)/day/body weight (g) (C) and energy consumption (kcal)/day/body weight (g) (D) after 8 weeks of diet. HC = Wistar fed a high-carbohydrate diet (n = 8); HF = Wistar high-fat diet (n = 8); HFHS = Wistar high-fat high-sugar diet (n = 6); GK = Goto-Kakizaki fed a high-carbohydrate diet (n = 10). The results are expressed as the mean ± S.D. (a) $p < 0.05$ compared with HC; (b) $p < 0.05$ compared with HF; (c) $p < 0.05$ compared with HFHS, using one-way ANOVA and Tukey's posttest.

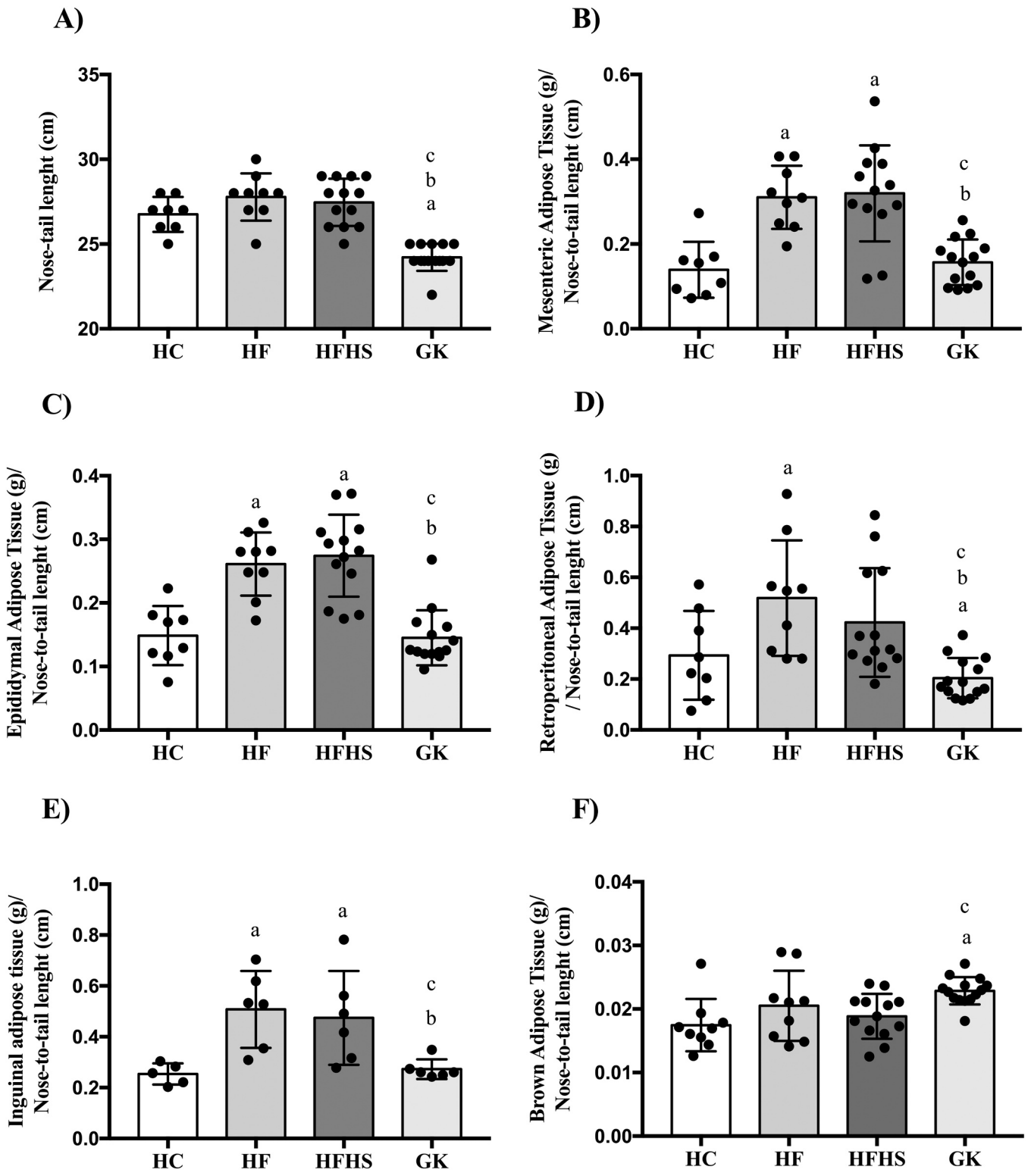

Fig. 3. Nose-to-tail length (A); Mesenteric adipose tissue (B); Epididymal adipose tissue (C); Retroperitoneal adipose tissue (D), inguinal adipose tissue (E) and brown adipose tissue (F). Adipose tissue depot weight was normalized by the animal's nose-to-tail length. HC = Wistar fed a high-carbohydrate diet (n = 8); HF = Wistar high-fat diet (n = 8); HFHS = Wistar high-fat high-sugar diet (n = 6); GK = Goto-Kakizaki fed a high-carbohydrate diet (n = 10). The results are expressed as the mean ± S.D. (a) $p < 0.05$ compared with HC; (b) $p < 0.05$ compared with HF; (c) $p < 0.05$ compared with HFHS, using one-way ANOVA and Tukey's posttest.

Fixed samples of interscapular BAT were dehydrated by sequentially increasing ethanol concentrations, diaphonized in xylene, and then embedded in paraffin. Slides were obtained containing 5-μm semiserial sections and stained with hematoxylin and eosin (HE). Slides with tissue pieces were placed in a microscopy chamber, images were acquired on a Nikon trinocular microscope (Nikon Eclipse, Tokyo, Japan), and a 40x objective was used. Five fields per section were acquired, four animals per group were used, and a total of 80 images per group were analyzed. Adipocyte quantitative and morphometric evaluations were performed using ImageJ/Fiji software (version 1.51r; NIH, Maryland, USA).

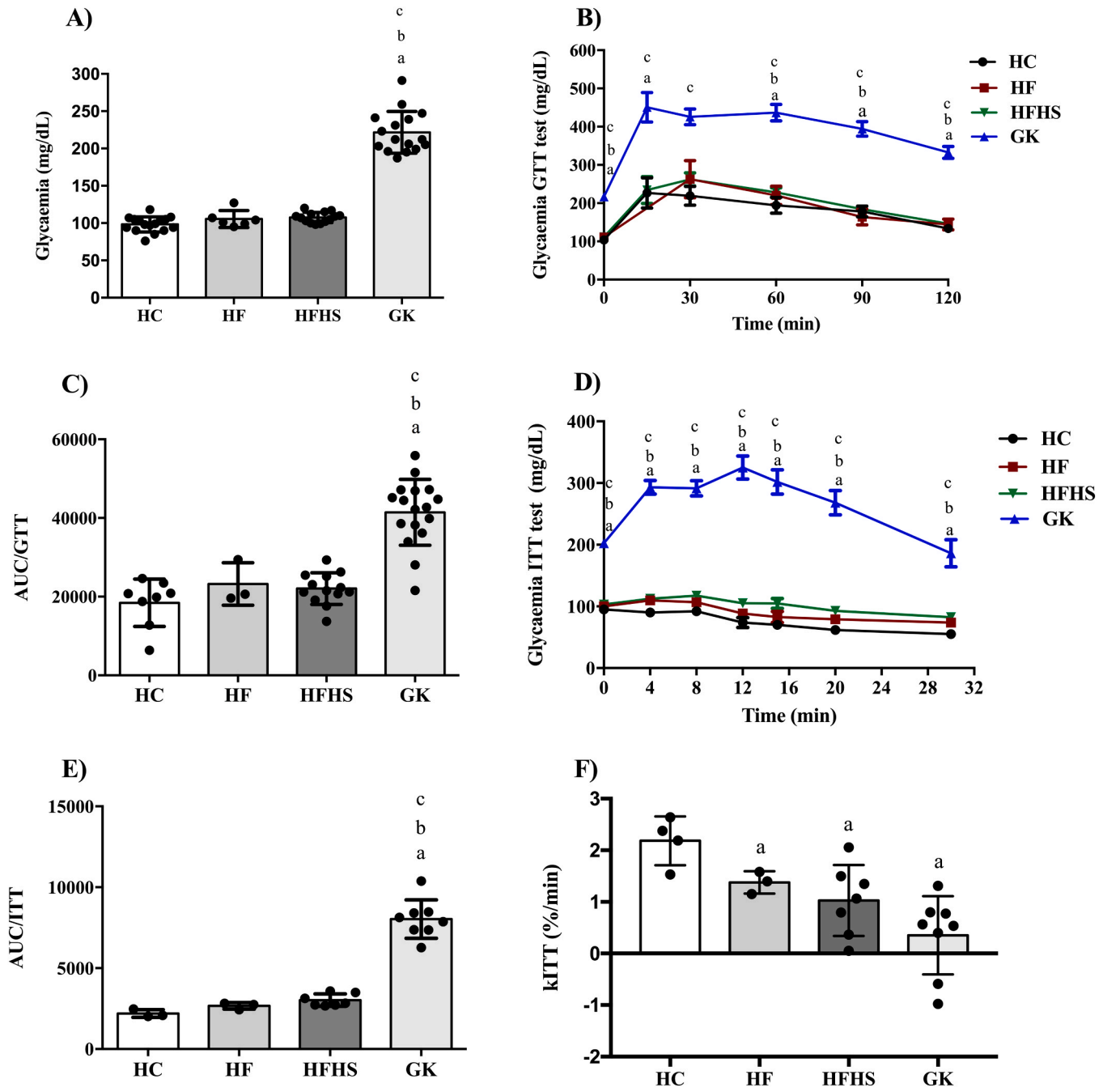

Fig. 4. Fasting glycemia (A**);** Glycemia measured during the glucose tolerance test (GTT) (B); area under curve (AUC) of glycemia measured during GTT (C); glycemia measured during the insulin tolerance test (ITT) (D); area under curve measured during ITT (E) and constant rate for ITT (kITT) (F) after 12 h fasting. HC = Wistar fed a high-carbohydrate diet (GTT n = 8; ITT n = 4, and kITT n = 4); HF = Wistar fed a high-fat diet (GTT and ITT n = 3; kITT n = 3); HFHS = Wistar fed a high-fat high-sugar diet (GTT n = 13; ITT and kITT n = 6); GK = Goto-Kakizaki fed a high-carbohydrate diet (GTT n = 17, ITT and kITT n = 8). The results are expressed as the mean ± S.D. (a) $p < 0.05$ compared with HC; (b) $p < 0.05$ compared with HF; (c) $p < 0.05$ compared with HFHS, using one-way ANOVA and Tukey's posttest.

2.11.1. Histological analysis

The images obtained were projected onto a computer screen and analyzed using ImageJ/Fiji software (version 1.51r; NIH, MD, USA). For quantitative analyses, due to numerous cells, the counting area (100 cm^2) was delimited using a system with inclusion and exclusion lines. Then, the adipocytes that touched the inclusion line were counted, and the adipocytes that crossed the exclusion line were not counted [27]. For morphometric analysis, 150 cells per group were measured to determine the adipocyte area, which was obtained in square micrometers (μm^2) [27].

2.12. Statistical analysis

The results are presented as the mean and standard deviation (S.D.). Statistical significance was assessed by *one-way* ANOVA or *two-way* ANOVA followed by the Bonferroni posttest or Tukey posttest (GraphPad Prism, version 7.0). The differences were considered to be statistically significant for $p < 0.05$.

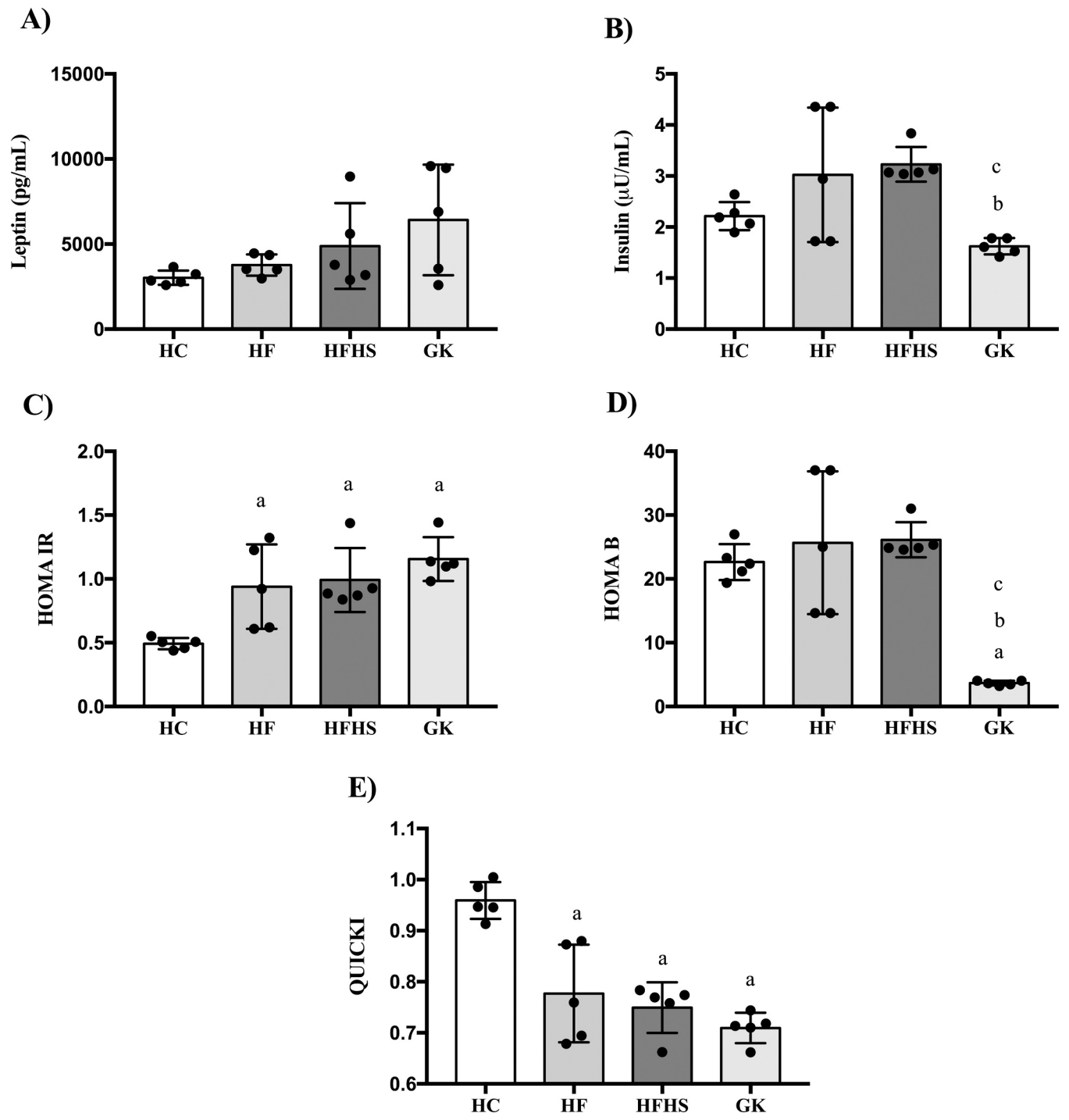

Fig. 5. Serum leptin levels measured at 16 weeks of age after 12 h fasting (A); Insulin serum levels at 16 weeks of age after 12 h fasting (B); HOMA-IR (C); HOMA-B (D) and QUICKI (E) indexes. HC = Wistar fed a high-carbohydrate diet (n = 5); HF = Wistar fed a high-fat diet (n = 5); HFHS = Wistar fed a high-fat high-sugar diet (n = 5); GK = Goto-Kakizaki fed a high-carbohydrate diet (n = 5). The results are expressed as the mean ± S.D. (a) $p < 0.05$ compared with HC; (b) $p < 0.05$ compared with HF; (c) $p < 0.05$ compared with HFHS, using one-way ANOVA and Tukey's posttest.

3. Results

All groups showed body weight gain during 8 weeks of diet, but the HF and HFHS groups showed higher ($p < 0.05$) body weights after 8 weeks of diet than the HC and GK groups (Fig. 1A). GK rats showed lower ($p < 0.05$) weight gain than HC, HF and HFHS rats (Fig. 1B).

Food intake and energy consumption were measured. When the values did not normalize, the HF and HFHS groups showed lower ($p < 0.05$) food intake than the HC group. The HFHS group also showed lower ($p < 0.05$) food intake than the HF and GK groups (Fig. 2A). When energy consumption was measured, HFHS rats consumed higher ($p < 0.05$) energy per day compared to HC and GK rats, which also consumed lower ($p < 0.05$) energy per day than HC and HF rats (Fig. 2B). However, when food intake and energy consumption were normalized per gram (g), GK rats showed increased ($p < 0.05$) food intake compared to HF and HFHS groups. The HF also showed decreased ($p < 0.05$) food intake compared to HC, and HFHS showed decreased ($p < 0.05$) compared to HC and HF, showing that the ingestion of

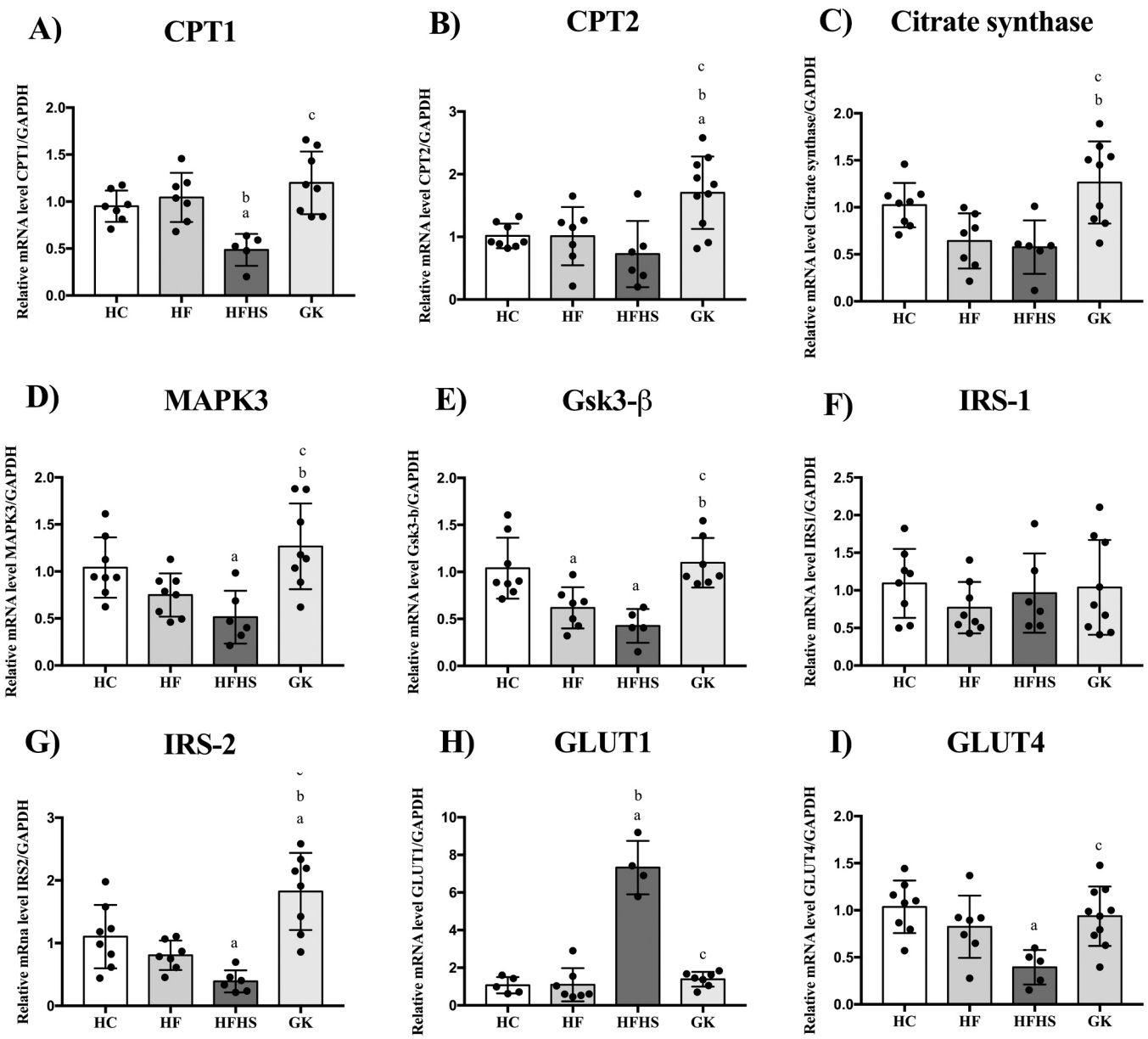

Fig. 6. Gene expression of CPT1 (A), CPT2 (B), citrate synthase (C), MAPK3 (D), Gsk3-β (E), IRS-1 (F), IRS-2 (G), GLUT1 (H), and GLUT4 (I) in the interscapular BAT of 16-week-old rats fed obesogenic diets (8 weeks). HC = Wistar fed a high-carbohydrate diet (n = 8); HF = Wistar fed a high-fat diet (n = 8); HFHS = Wistar fed a high-fat high-sugar diet (n = 6); GK = Goto-Kakizaki fed a high-carbohydrate diet (n = 10). The results are expressed as the mean ± S.D. (a) $p < 0.05$ compared with HC; (b) $p < 0.05$ compared with HF; (c) $p < 0.05$ compared with HFHS, using one-way ANOVA and Tukey's posttest. Carnitine palmitoyltransferases 1 and 2 (CPT1 and 2); mitogen-activated protein kinase 3 (MAPK3); glycogen synthase kinase 3 β (Gsk3-*β*); insulin receptor substrates 1 and 2 (IRS-1 and 2); glucose transporters 1 and 4 (GLUT1 and 4).

condensed milk led to a reduced food intake (Fig. 2C). No difference was observed between the groups in measurement of energy consumption when normalized per gram (g) (Fig. 2D).

GK rats showed decreased nose-to-tail length ($p < 0.05$) compared to all groups (Fig. 3A), lower ($p < 0.05$) adipose tissue depots: retroperitoneal compared to all groups (Fig. 3D), mesenteric, epididymal and inguinal compared to HF and HFHS (Fig. 3B, C, and E), and increased mass weight ($p < 0.05$) of brown adipose tissue compared to HC and HFHS (Fig. 3F). Higher quantities of lipids contained in the HF and HFHS diets induced an increased mass weight ($p < 0.05$) of mesenteric, epididymal, and inguinal adipose tissue compared to HC (Fig. 3B, C, and E). HF diet induced an increased mass weight ($p < 0.05$) of retroperitoneal adipose tissue compared to HC (Fig. 3D).

GK rats showed increased ($p < 0.05$) fasting glucose levels compared to all groups (Fig. 4A). After challenge with glucose (2 g/kg of body weight) or insulin (0.50 UI/of body weight), GK rats showed an increased ($p < 0.05$) glucose blood levels and higher area under the curve compared to HC, HF, and HFHS (Fig. 4B, C, D, and E). HF, HFHS, and GK rats showed significantly lower insulin sensitivity than HC rats ($p < 0.05$), as indicated by the kITT (Fig. 4F).

We measured leptin and inulin serum levels. No difference was observed between the groups in leptin levels (Fig. 5A). After 12 h of fasting, GK rats presented lower ($p < 0.05$) insulin levels compared to HF and HFHS (Fig. 5B). Next, to validate the results shown above, HOMA-IR, HOMA B, and QUICKI were calculated. HOMA-IR showed an increase ($p < 0.05$) in HF, HFHS, and GK rats compared to HC (Fig. 5C), indicating IR in these animals. HOMA B is clearly altered in GK rats, showing a decrease ($p < 0.05$) compared to all groups (Fig. 5D). QUICKI

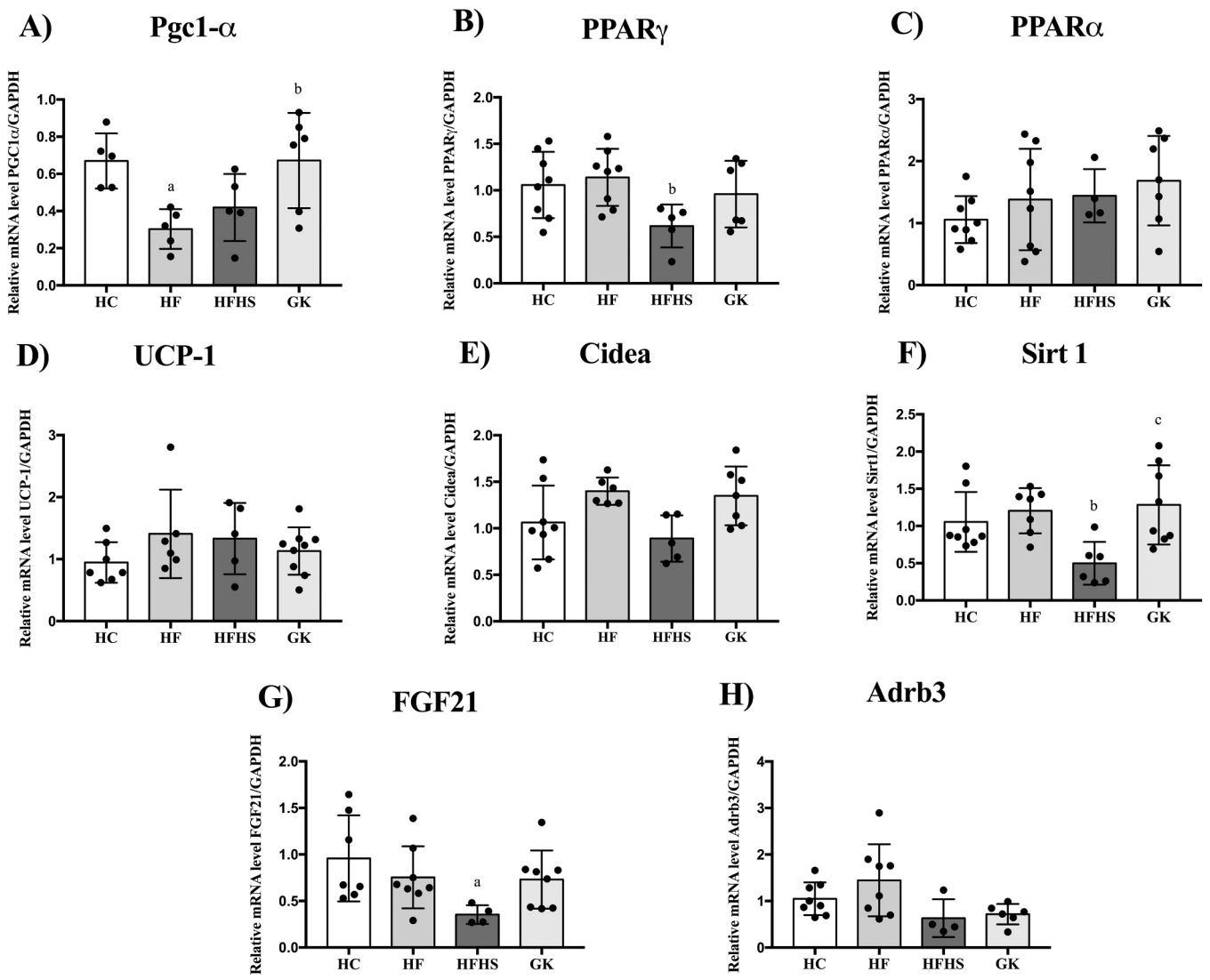

Fig. 7. Gene expression of Pgc1-*α* (A), PPAR*γ* (B), PPAR*α* (C), UCP-1 (D), Cidea (E), Sirt1 (F), FGF21 (G), and Adrb3 (H from interscapular BAT of rats of 16 weeks of age fed obesogenic diets (8 weeks). HC = Wistar fed a high-carbohydrate diet (n = 8); HF = Wistar fed a high-fat diet (n = 8); HFHS = Wistar fed a high-fat high-sugar diet (n = 6); GK = Goto-Kakizaki fed a high-carbohydrate diet (n = 10). The results are expressed as the mean ± S.D. (a) $p < 0.05$ compared with HC; (b) $p < 0.05$ compared with HF; (c) $p < 0.05$ compared with HFHS, using one-way ANOVA and Tukey's posttest. Peroxisome Proliferator-Activated Receptor Gamma Coactivator 1 Alpha (Pgc1-α); Peroxisome Proliferator-Activated Receptor Gamma (PPARγ); Peroxisome Proliferator-Activated Receptor alpha (PPARα); uncoupling protein (UCP1); cell death-inducing DNA fragmentation factor alpha-like effector A (Cidea); Sirtuin 1 (Sirt1); Fibroblast growth factor 1 (FGF21); and beta 3 adrenergic receptor (Adrb3).

showed a decrease ($p < 0.05$) in HF, HFHS, and GK rats compared to HC (Fig. 5E), indicating impaired insulin sensitivity in these animals.

Genes involved in BAT metabolism were identified at interscapular depots. We observed increased ($p < 0.05$) mRNA expression of genes involved in fatty acids oxidation in BAT from GK of carnitine palmitoyltransferase 1 (CPT1) when compared to HFHS group (Fig. 6A), carnitine palmitoyltransferase 2 (CPT2) when compared to all groups (Fig. 6B), and citrate synthase when compared to HF and HFHS group (Fig. 6C); however, the CPT1 from BAT of HFHS group showed decreased ($p < 0.05$) mRNA expression when compared to HC and HF groups (Fig. 6A). BAT from GK rats showed increased ($p < 0.05$) mRNA expression of genes involved in the insulin signaling pathway, mitogen-activated protein kinase 3 (MAPK3) and glycogen synthase kinase 3 β (Gsk3-*β)* when compared to HF and HFHS group (Fig. 6D and E), insulin receptor substrate 2 (IRS-2) when compared to all groups (Fig. 6G); however, the MAPK3 from BAT of HFHS group, and Gsk3-*β* from BAT of HF and HFHS groups were decreased ($p < 0.05$) when compared to HC (Fig. 6D and E), as well as the IRS-2 from BAT of HFHS when compared to HC (Fig. 5G). No difference was observed between the groups in the mRNA expression of insulin receptor substrate 1 (IRS-1) (Fig. 6F). We also analyzed the mRNA expression of genes involved in glucose metabolism, where the BAT from GK rats showed increased ($p < 0.05$) mRNA expression of glucose transporter 4 (GLUT4) when compared to HFHS group, which showed decreased ($p < 0.05$) mRNA expression when compared to HC group (Fig. 5I). However, the HFHS group showed increased ($p < 0.05$) expression of glucose transporter 1 (GLUT1) compared to all groups (Fig. 6H).

We evaluated the gene expression of genes involved in transcriptional regulation and BAT metabolism. The expression levels of genes involved in transcriptional regulation, such as peroxisome proliferator-activated receptor-gamma coactivator α (Pgc1-α), were increased ($p < 0.05$) in the BAT of GK rats compared to the HF group and were also decreased ($p < 0.05$) compared to the HC group (Fig. 7A). The mRNA expression of peroxisome proliferator-activated receptor γ (PPARγ) was decreased ($p < 0.05$) in the BAT of GK rats compared to the HF group (Fig. 7B). No difference was observed between the groups in the mRNA

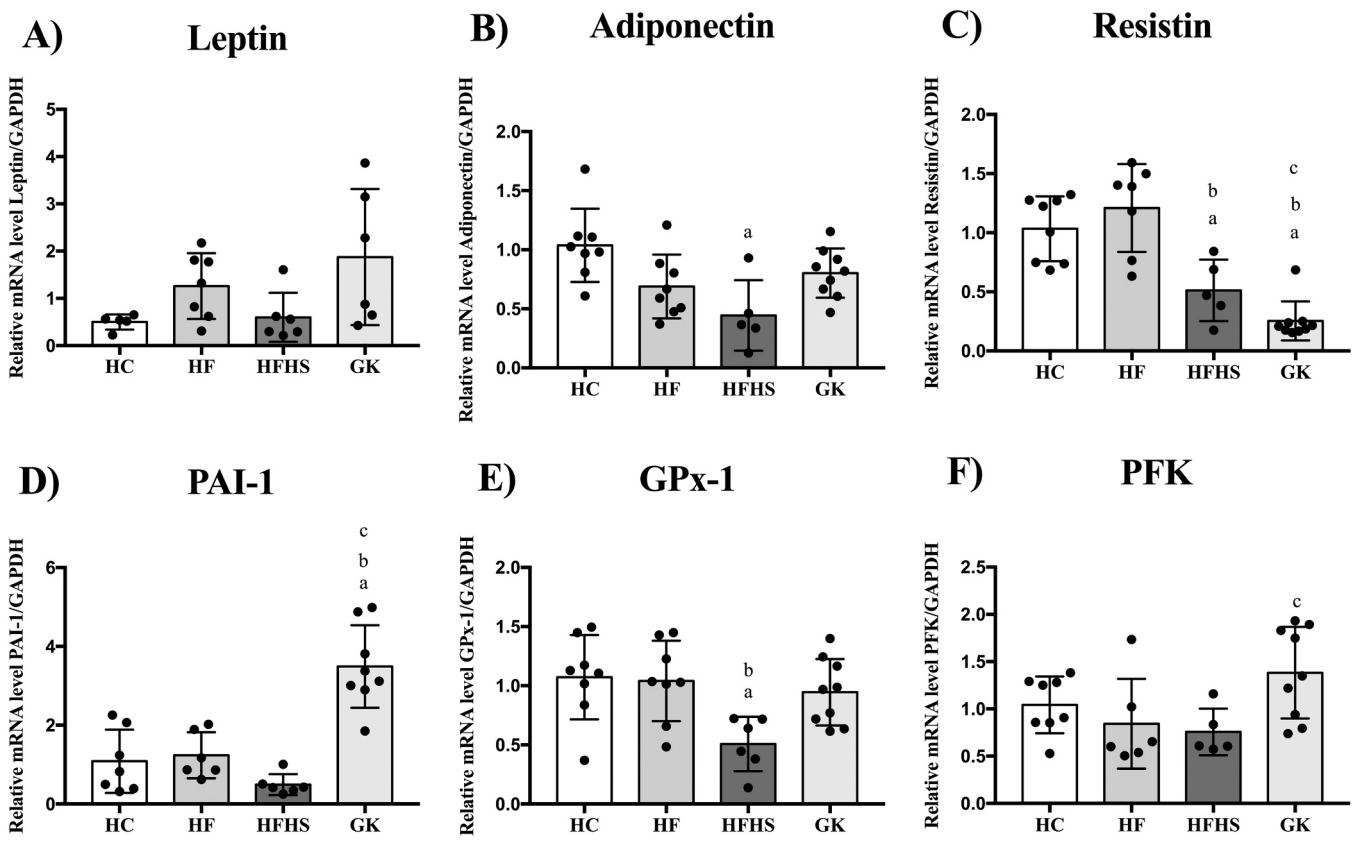

Fig. 8. Gene expression of leptin (A), adiponectin (B), resistin (C), PAI-1 (D), GPx-1 (E), and PFK in the interscapular BAT of 16-week-old rats fed obesogenic diets (8 weeks). HC = Wistar fed a high-carbohydrate diet (n = 8); HF = Wistar fed a high-fat diet (n = 8); HFHS = Wistar fed a high-fat high-sugar diet (n = 6); GK = Goto-Kakizaki fed a high-carbohydrate diet (n = 10). The results are expressed as the mean ± S.D. (a) $p < 0.05$ compared with HC; (b) $p < 0.05$ compared with HF; (c) $p < 0.05$ compared with HFHS, using one-way ANOVA and Tukey's posttest. Plasminogen activator inhibitor-1 (PAI-1); glutathione peroxidase 1 (GPx-1), and phosphofructokinase (PFK).

expression of peroxisome proliferator-activated receptor α (PPARα) (Fig. 7C). The expression levels of genes encoding established markers of BAT activity, such as Sirt1, were increased ($p < 0.05$) in GK rats compared to HFHS rats and were decreased ($p < 0.05$) compared to HF rats (Fig. 7F). Although we did not observe any difference between groups in Adrb3 gene expression, the β3 adrenergic receptor, there was a tendency towards a decrease expression in GK rats compared to HF rats (Fig. 7H). The mRNA expression of fibroblast growth factor 21 (FGF21), which is also secreted and released from BAT, named "batokine", was decreased ($p < 0.05$) in the BAT of the HFHS group compared to the HC group (Fig. 7G). We did not observe any differences between the groups in the mRNA expression of thermogenic genes such as UCP-1 and cell death-inducing DNA fragmentation factor alpha-like effector A (Cidea) (Fig. 7D and E).

We also evaluated the gene expression of adipogenic genes, inflammation and biogenesis of obesity in BAT at interscapular depots. No difference was observed between the groups in mRNA expression of leptin; however, there was a tendency towards an increase expression in GK rats compared to HF and HFHS groups (Fig. 8A). BAT from GK rats showed increased mRNA expression of plasminogen activator inhibitor-1 (PAI-1) compared to all groups (Fig. 8D). HFHS showed decreased mRNA expression glutathione peroxidase 1 (GPx1) compared to HC and HF groups and decreased mRNA expression of phosphofructokinase (PFK) compared to GK rats (Fig. 8E and F). We showed decreased ($p < 0.05$) mRNA expression of resistin in GK rats compared to all groups (Fig. 8C). The HFHS group showed decreased ($p < 0.05$) mRNA expression of adiponectin compared to HC and of resistin compared to HC and HF (Fig. 8B and C).

Next, to validate the observation made above, the total protein amount of thermogenic protein and the batokine were measured from interscapular BAT of rats by Western blotting. Although no difference was observed between the groups in UCP1 protein levels, there was a tendency towards a decrease UCP1 protein levels in GK rats compared to HF rats (Fig. 9A and B). Wistar fed a HFHS diet showed decreased ($p < 0.05$) FGF21 protein levels compared to HF rats (Fig. 9C and D), showing a reduced effect due to the diet macronutrient combination.

To investigate glucose uptake from the interscapular BAT of rats fed obesogenic diets. The glucose uptake was measured by ^{18}F-FDG PET-CT. Here, the basal BAT glucose uptake did not show significant differences between the groups (Fig. 10A). After adrenergic stimulation by intravenous CL 316,243 administration, GK rats showed lower ($p < 0.05$) ^{18}F-FDG uptake in BAT than HC rats. However, in the comparison between basal and stimulated conditions (after CL316,243 intravenous injection), increased ($p < 0.05$) ^{18}F-FDG uptake was observed only in the HC group by 4.5-fold (Fig. 10A). Representative images of ^{18}F-FDG uptake by BAT are presented in Fig. 10B.

Finally, histological analysis was performed at the interscapular BAT of rats fed obesogenic diets. Staining with HE interscapular BAT from GK animals demonstrated that increased adipocyte areas showed great lipid accumulation by qualitative analyses when compared to all groups (Fig. 11A). Morphologically, interscapular BAT from GK animals had lower ($p < 0.05$) cell density compared to all groups, and HF and HFHS rats showed lower ($p < 0.05$) cell density when compared to HC (Fig. 11B). The interscapular BAT from GK animals showed a higher ($p < 0.05$) adipocyte area than the interscapular BAT of all groups, and HF and HFHS animals showed higher ($p < 0.05$) adipocyte areas than HCs (Fig. 11C).

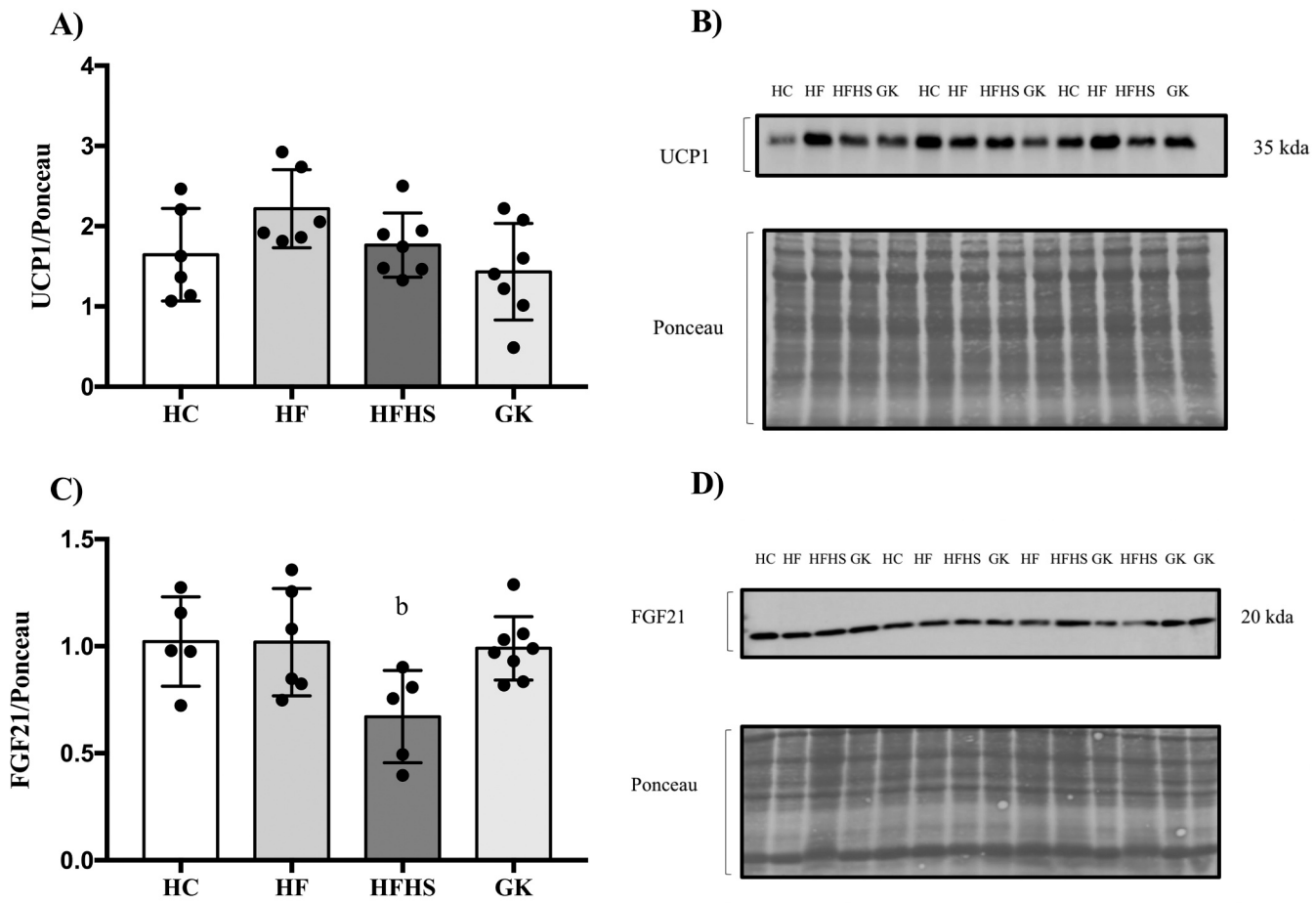

Fig. 9. Total protein amount from interscapular BAT of 16-week-old rats fed obesogenic diets (8 weeks) by Western blotting. Quantification of UCP1 protein amount A), representative immunoblot showing UCP1 protein with Ponceau staining as a loading control (B), quantification of FGF21 protein amount (C), and representative immunoblot showing FGF21 protein with Ponceau staining as a loading control (D). HC = Wistar fed a high-carbohydrate diet (n = 6); HF = Wistar fed a high-fat diet (n = 6); HFHS = Wistar fed a high-fat high-sugar diet (n = 7); GK = Goto-Kakizaki fed a high-carbohydrate diet (n = 8). The results are expressed as the mean ± S.D. (a) $p < 0.05$ compared with HC; (b) $p < 0.05$ compared with HF; (c) $p < 0.05$ compared with HFHS, using one-way ANOVA and Tukey's posttest.

4. Discussion

T2D has been mainly associated with obesity; however, it has been also associated without obesity, mainly in Asian population [4,28,29]. Then, understand the differences between obese and lean models of insulin resistance, and understanding the regulatory mechanisms responsible for the metabolic alterations is therefore essential to find alternative options to minimize the consequences and progression of insulin resistance. BAT has been proposed as a target to treat obesity and T2D, due to the high metabolic activity to produce heat. Then, it becomes important to elucidate the different models of IR at varying intensities on the underlying mechanisms of BAT dysfunction. This study is the first to investigate BAT function in genetic T2D and lean model GK rats. Different rat models have been used to investigate the IR mechanisms aiming to translate to human disorders. Herein, we used models of obese Wistar rats induced by obesogenic diets (classic models in the literature to study IR induced by obesity), and GK rats, a genetic model of IR, which is used as a model to investigate the complications related to T2D without obesity. Herein, using these different models of IR at varying intensities, associated or not with obesity, to investigate the underlying mechanisms of BAT dysfunction in these models, we expect that our findings help other researchers to understand the effects of different IR models on the impaired BAT function [30,31].

The HF and HFHS diets induced obesity, as demonstrated by the mass expansion of WAT depots according to previous studies [4,32]. In addition, studies have demonstrated hyperphagia in GK rats when compared to Wistar rats, which was corroborated by our finding showing an increase in food intake per g [33]. Obesogenic diets present high amounts of fat and/or sugar in their composition, and they have been shown to be associated with impaired insulin sensitivity [4,34]. We could not observe any difference between lean and obese Wistar rats in the glucose tolerance test, while GK rats presented a deep impairment in this parameter. All groups (obese Wistar rats and GK rats) displayed impaired sensibility to insulin as demonstrated by the glucose decay during ITT in comparison to the control group. In a previous work, we demonstrated that obese Wistar rats present hyperinsulinemia during GTT, which is needed to keep blood glucose to normal levels [1]. These findings suggest that obese rats present normal glucose tolerance due to increased insulin secretion during GTT, indicating that these animals are insulin resistant, as demonstrated by the ITT. The GK rats, by the other hand, are unable to compensate the insulin resistance with increased hormone secretion, exhibiting elevated glucose intolerance (GTT) and reduced insulin sensitivity (ITT). To confirm our findings, we additionally measured the insulin plasma levels during fasting and calculate some indexes related to the hormone response. We could not observe any significant difference in the insulin plasma levels among the groups, but the obese Wistar rats presented a tendency of increase and the GK rats a tendency of decrease. Obese Wistar and GK rats presented elevated HOMA-IR (insulin resistance index) and reduced QUICKI (insulin sensitivity index). There was no difference in HOMA-beta between HC group and obese Wistar rats, suggesting that these animals have a normal beta cell function and thus they can compensate the insulin

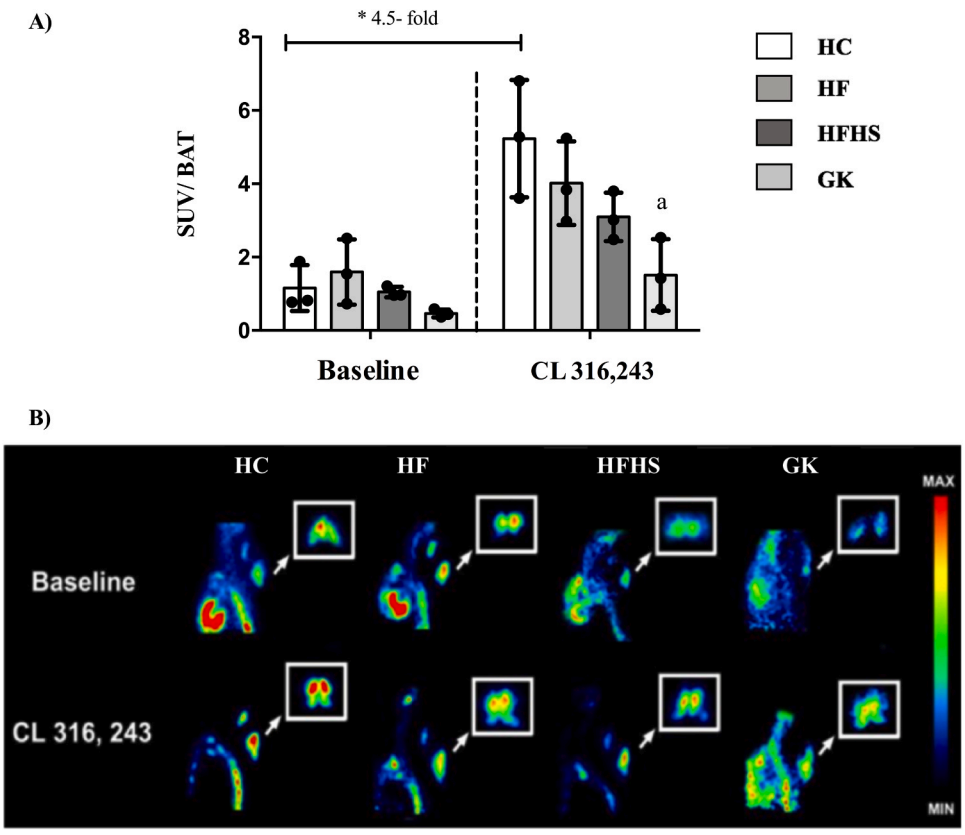

Fig. 10. Interscapular brown adipose tissue activity evaluated by ^{18}F-FDG uptake. Graphs represent ^{18}F-FDG BAT uptake after saline and CL316,243 (A) and representative images of ^{18}F-FDG BAT uptake from rats injected with saline (baseline) or CL316,243 (B). HC = Wistar fed a high-carbohydrate diet (n = 3); HF = Wistar high-fat diet (n = 3); HFHS = Wistar high-fat high-sugar diet (n = 3); GK = Goto-Kakizaki fed a high-carbohydrate diet (n = 3). The results are expressed as the mean ± S.D. (a) $p < 0.05$ compared with HC; (b) $p < 0.05$ compared with HF; (c) $p < 0.05$ compared with HFHS, using two-way ANOVA and Tukey's posttest.

resistance by increasing the hormone production, resulting in a normal glucose tolerance during GTT. The GK rats, by the other hand, demonstrated a pronounced decrease in the HOMA-beta, suggesting that the beta cell function is highly impaired in these animals, leading to a deep glucose intolerance during GTT. Thus, using these different models of IR, lean and obese animals, we could investigate the underlying mechanisms of BAT dysfunction, since several strategies have been hypothesized to target BAT in different conditions of IR. Further studies are required to investigate potential strategies to improve BAT function in the obese Wistar and GK rats, based on our findings, aiming to reduce or prevent IR in these models. Here, we observed an increase in BAT mass from GK rats. However, this increase in BAT mass cannot be directly associated with BAT activity, since an increase has also been observed under inactivity conditions as a result of lipid accumulation [35–37].

Fatty acid metabolism is important during thermogenesis since the fatty acid metabolism is required for UCP1 proton transport activity in BAT [38,39]. BAT has been described as having the highest fatty acid oxidation rate [40,41]. The enzymes CPT1 and CPT2 are related to fatty acid transport into the mitochondrial membrane. Numerous studies have shown a decrease in CPT1 activity in the BAT of diabetic rats [42]. Immortalized brown adipocytes of rats have shown that CPT1 leads to increased fatty acid oxidation and UCP1 protein levels [41]. Mice with adipose-specific loss of CPT2 have shown decreased BAT thermogenic activity [43]. In addition, lower citrate synthase activity, a key mitochondrial enzyme, has been associated with impaired glucose tolerance [44,45]. Our findings suggest enhanced BAT fatty acid oxidation in GK rats and impaired BAT fatty acid oxidation in HFHS rats.

Improving the insulin receptor signaling pathway is a mechanism by which BAT efficiently takes up glucose [46]. IRS-2 is associated with IR and impairment of sympathetic innervation [47]. Studies have shown decreased insulin-induced glucose uptake in preadipocytes derived from IRS-2 knockout (KO) mice [47]. In addition, improvement of sympathetic nervous function in BAT is mediated by MAPK3 [48]. However, low Gsk3-β activity is associated with greater thermogenesis activity and oxygen consumption in response to adrenergic stimuli [49]. Additionally, stimulation of glucose uptake is considered an important parameter for measuring BAT activity [9,50]. In brown adipocytes, adrb3-stimulated glucose uptake is mediated by an increase in cAMP, which leads to the *de novo* synthesis of GLUT1 [51]. In this regard, enhanced glucose tolerance and insulin sensitivity have been demonstrated in mice overexpressing Sirt1 [52]. In the present study, although increased expression of genes is involved in insulin signaling and glucose transporters in GK rats, it was not sufficient to enhance glucose uptake in these animals.

UCP1 has been well documented to be a thermogenic protein expressed specifically in brown and beige adipocytes [9,55,56]. Numerous studies have associated the lack of UCP1 with impaired BAT mitochondrial function and lower energy expenditure [57,58], indicating impaired thermogenic activity in GK rats, whereas rats fed an HF diet have shown increased thermogenic activity in response to a high amount of fat in the diet composition, which has been associated with an increased fatty acid combusting capacity [59,60]. Additionally, BAT plays an endocrine role by acting as a secretory organ; it can release and secrete brown adipokines, commonly named "batokines", such as FGF21 [61–63]. BAT seems to be involved in glucose uptake improvement and induces UCP1 and Pgc1-α [64,65]. Recently, Keipert et al. [66] showed increased FGF21 mRNA levels in the BAT of UCP1-KO mice fed an HF diet. In the present study, we also revealed higher expression of FGF21 and Pgc1-α in BAT in GK rats but a reduction in expression in rats fed an HFHS diet.

Adipokines are secreted and released by adipocytes, having systemic effects [67–69]. The adipokines may have autocrine, paracrine and endocrine functions, acting in several organs, including the own adipose tissue [69,70]. They can shift to pro-inflammatory state in response to nutritional and hormonal modifications, such as obesity and type 2 diabetes [69–71]. Both adipokine synthesis and levels have been associated in obesity. Although the findings of adipokine mRNA expression are limited, it has been suggested a clear relationship between adipokine

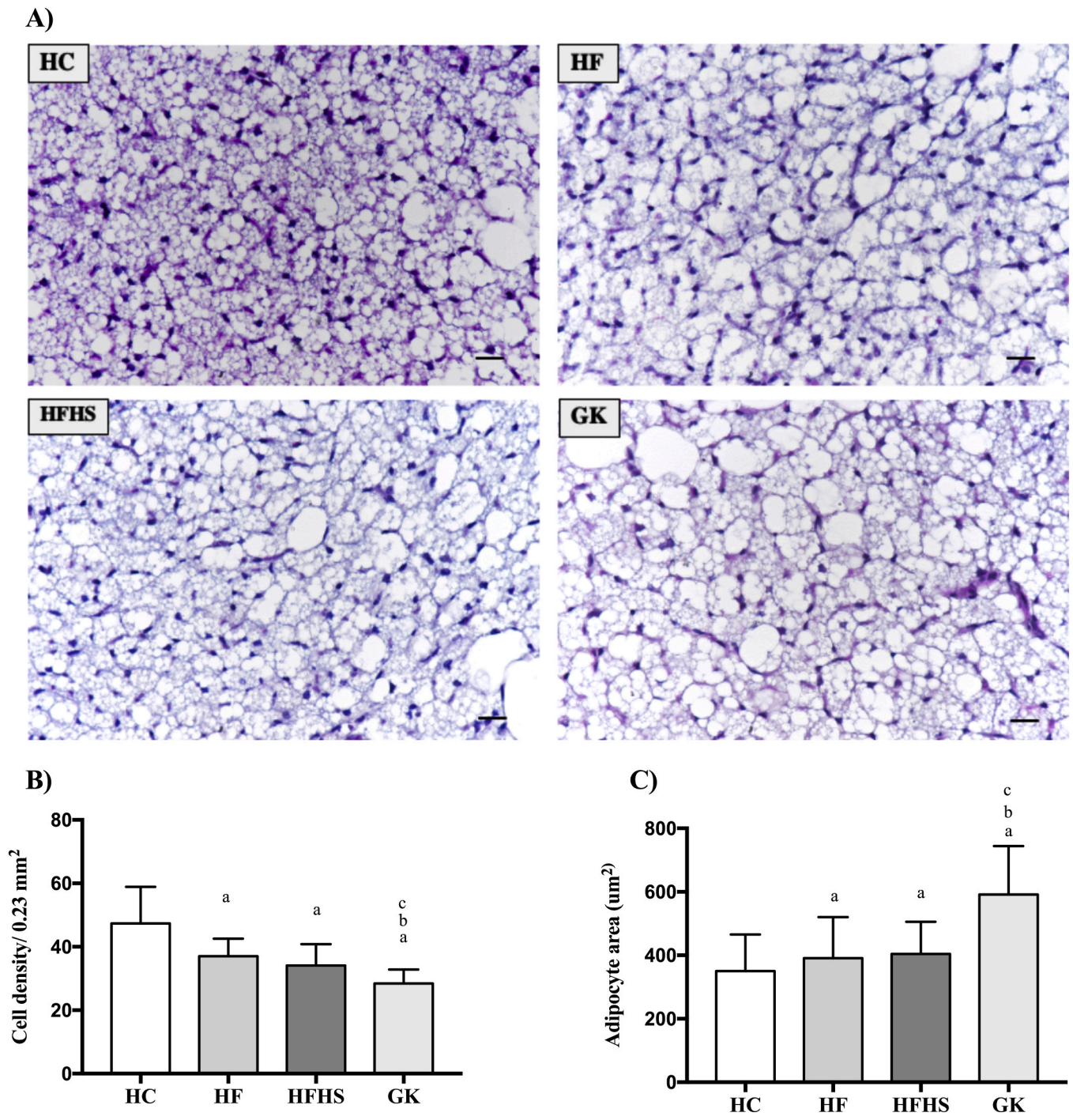

Fig. 11. Histological analysis of interscapular BAT stained with HE. Illustration of interscapular BAT morphology (A); considered cell density; objective= 40× and bar = 20 μm (B); adipocyte area (μm^2) measured in 150 cells per animal (C). HC = Wistar rats fed a high-carbohydrate diet (n = 3); HF = Wistar rats high-fat diet (n = 4); HFHS = Wistar rats high-fat high-sugar diet (n = 4); GK = Goto-Kakizaki fed a high-carbohydrate diet (n = 4). The results are expressed as the mean ± S.D. (a) $p < 0.05$ compared with HC; (b) $p < 0.05$ compared with HF; (c) $p < 0.05$ compared with HFHS, using one-way ANOVA and Tukey's posttest.

expression and plasma levels, as reported in a previous study [72]. Leptin is secreted mainly by subcutaneous WAT, and obesity and IR have been associated with their lack and/or resistance [68,73]; however, leptin is not a thermogenic hormone [37] and it has been also found increased in obese and diabetic patients [74] to confirm our findings concerning mRNA expression of leptin, we evaluated the plasma leptin content. Overall, our findings were similar between plasma levels and BAT mRNA expression of leptin; there was no significant differences among the four groups, but we observed a tendency of increase in obese rats and mainly in GK rats. It is important to highlight that the adipokines are produced by all types of adipocytes, not only BAT. Our results herein suggest BAT adipokine expression can have an important contribution and reflect the plasma adipokine levels. Adiponectin has been associated with a decreased in obese patients, although its action on BAT is not entirely clear. Adiponectin has been reported to be involved in thermogenesis [74,75]. Resistin, another adipokine, is associated with the inflammatory process [76]. BAT of GK rats showed upregulation of genes associated with IR and obesity. Therefore, higher expression of leptin in these animals could be associated with a diabetes phenotype and high lipid storage in BAT depots.

It is well known that the sympathetic nervous system regulates brown adipose tissue activity through β3-adrenergic receptors (adrb3), stimulating lipolysis and thermogenesis activation [9,77,78]. Several groups have demonstrated that adrb3 agonists induce thermogenesis. In our study, because our rats were isoflurane anesthetized, there was abolition in BAT-derived thermogenesis [79–81]. Thus, we measured only glucose uptake independently of thermogenesis activity. Additionally, treatment with selective adrb3 agonist, CL 316,243, in rodents, has demonstrated an improvement in glucose uptake. Glucose uptake was evaluated by ^{18}F-FDG uptake in BAT using a PET-CT scan when visualizing areas of increased tracer uptake [50]. Although PET-FDG images do not exclusively show BAT thermogenesis, they may show BAT adrenergic activity since the adrenergic signaling pathway mediates glucose uptake [81]. Accordingly, thermogenesis and metabolic activity have been shown to be associated with increased BAT glucose uptake [82,83]. Previous studies demonstrated a reduction in glucose uptake in the BAT of diabetic mice and obese humans [84,85]. Lapa et al. [83] observed, in Zucker diabetic rats, loss of BAT function identified by decreased ^{18}F-FDG uptake, which together with a histological analysis showed morphologic transition from BAT to white adipose tissue. Our findings indicate impaired glucose uptake of BAT in GK rats under β3-adrenergic stimulation. The lack of adrb3 in mice leads to an impaired metabolic rate, contributing to obesity induced by high-fat diet [86]. In addition, reduction of adrb3 leads to an impaired intracellular cAMP level and PKA activity [53,54]. Here, we aimed to evaluated the adrb3 response in BAT of different insulin-resistant animals. Since adrb3 stimulates PKA activity and cAMP production and we found an impairment in the expression of this protein in BAT from GK rats, as well as a reduction in beta-3 agonist response, we could hypothesize this pathway is greatly impaired and the potential mechanism involved in BAT dysfunction in these animals.

One of the major differences between WAT and BAT has been described as intracellular lipid droplet morphology. BAT displays a small and multilocular lipid droplet, while WAT displays a single lipid droplet [83,87,88]. In the BAT of Zucker rats, a model of T2D rats presented an increase in adipocyte size compared to obese and control animals [83]. Additionally, in obese mice, lipid accumulation measured by histology has been associated with metabolic inactivity [37,89]. Correspondingly, our data showed lower cell density and higher adipocyte area in interscapular BAT of GK rats,indicating lipid accumulation.

In summary, obesogenic diets containing high amounts of fat and/or sugar induced obesity in Wistar rats; however, no difference in body weight or IR was observed between the rats fed the HF and HFHS diets. In spite of that lack of difference, the ingestion of the combination HFHS diet intensified the impairment in BAT function compared to a HF diet individually. Additionally, although our results showed increased mRNA expression of genes that are involved in fatty acid oxidation and insulin signaling pathways, these alterations were not enough to enhance BAT activity. Furthermore, impaired BAT function was also associated with a reduced cell density and elevated adipocyte area, indicating increased lipid droplet storage in interscapular BAT depots, and impaired BAT function was also congruent with increased leptin mRNA expression, which is correlated with adiposity. Herein, we observed that IR conditions in GK animals intensified the impairment of the beta-adrenergic response. Therefore, this impairment could suggest an increased expression of genes cited above, acting as a compensatory mechanism. Thus, our data suggest a transition from BAT to WAT, a process named “whitening”, in GK rats. Further studies are necessary to understand the mechanism and genes involved in the lean phenotype in the GK model, mainly in different adipose tissues, to understand why these animals have impaired accumulation of fat depots.

Declarations

The study was carried out in compliance with the ARRIVE guidelines and regulations.

Limitations

In addition to the constant temperature at 23 ± 2 °C, we did not maintain the rats at thermoneutrality (28 ± 2 °C), and we did not evaluate cold-induced BAT activity (4 °C).

CRediT authorship contribution statement

TDAS, LNM, TCAL, RBB, RG, TCPC, RC, and SMH designed the research and wrote the manuscript. TDAS, LNM, JNBP, LER, ALA, MVMS, VLSD, AACS, CPBSF, GNMN, and SMH performed the experimental protocols and analyzed the data. JNBP, GNMN, RBB, RG, TCPC, RC, and SMH helped in data interpretation and presentation. All authors critically revised and approved the final version of the manuscript.

Conflict of interest statement

The authors declare that there are no conflicts of interest.

Data Availability

The data that support the findings of this study are available from the corresponding author upon reasonable request.

Acknowledgments

The authors gratefully acknowledge the Laboratory of Nuclear Medicine of the University of São Paulo (LIM-43) for the supported PET-CT analysis. We thank the following financial support: São Paulo State Research Foundation – FAPESP (2016/14529-1; 2018/18815-4; 2018/09868-7; 2019/25936-5), National Council for Scientific and Technological Development – CNPq (303753/2015-3), and Coordination for the Improvement of Higher Education Personnel – CAPES (88881.068515/2014-01).

References

[1] W.M.T. Kuwabara, A.C. Panveloski-Costa, C. Yokota, J. Pereira, J.M. Filho, R. P. Torres, S.M. Hirabara, R. Curi, T.C. Alba-Loureiro, Comparison of Goto-Kakizaki rats and high fat diet-induced obese rats: are they reliable models to study Type 2 Diabetes mellitus? PLOS One 12 (12) (2017), 0189622.
[2] S.E. Kahn, M.E. Cooper, S. Del Prato, Pathophysiology and treatment of type 2 diabetes: perspectives on the past, present, and future, Lancet 383 (9922) (2014) 1068–1083.
[3] T.U. Maioli, J.L. Gonçalves, M.C. Miranda, V.D. Martins, L.S. Horta, T.G. Moreira, A.L. Godard, A.F. Santiago, A.M. Faria, High sugar and butter (HSB) diet induces obesity and metabolic syndrome with decrease in regulatory T cells in adipose tissue of mice, Inflamm. Res 65 (2) (2016) 169–178.
[4] L.N. Masi, A.R. Martins, A.R. Crisma, C.L. do Amaral, M.R. Davanso, T. Serdan, R. da Cunha de Sá, M.M. Cruz, M. Alonso-Vale, R.P. Torres, J. Mancini-Filho, J. Pereira, M.M. da Silva Righetti, E.A. Liberti, S.M. Hirabara, R. Curi, Combination of a high-fat diet with sweetened condensed milk exacerbates inflammation and insulin resistance induced by each separately in mice, Sci. Rep. 7 (1) (2017) 3937.
[5] S. Moreno-Fernández, M. Garcés-Rimón, G. Vera, J. Astier, J.F. Landrier, M. Miguel, High fat/high glucose diet induces metabolic syndrome in an experimental rat model, Nutrients 10 (2018) 10.
[6] C.J. Bailey, A.A. Tahrani, A.H. Barnett, Future glucose-lowering drugs for type 2 diabetes, Lancet Diabetes Endocrinol. 4 (4) (2016) 350–359.
[7] X. Yang, G.T. Ko, W.Y. So, R.C. Ma, L.W. Yu, A.P. Kong, H. Zhao, C.C. Chow, P. C. Tong, J.C. Chan, Associations of hyperglycemia and insulin usage with the risk of cancer in type 2 diabetes: the Hong Kong diabetes registry, Diabetes 59 (5) (2010) 1254–1260.
[8] U.P. Gujral, M.B. Weber, L.R. Staimez, K. Narayan, Diabetes among non-overweight individuals: an emerging public health challenge, Curr. Diabetes Rep. 18 (8) (2018) 60.
[9] B. Cannon, J. Nedergaard, Brown adipose tissue: function and physiological significance, Physiol. Rev. 84 (1) (2004) 277–359.
[10] L.A. Foellmi-Adams, B.M. Wyse, D. Herron, J. Nedergaard, R.F. Kletzien, Induction of uncoupling protein in brown adipose tissue. Synergy between norepinephrine and pioglitazone, an insulin-sensitizing agent, Biochem. Pharm. 52 (5) (1996) 693–701.
[11] S. Enerbäck, Human brown adipose tissue, Cell Metab. 11 (4) (2010) 248–252.
[12] J. Nedergaard, B. Cannon, The changed metabolic world with human brown adipose tissue: therapeutic visions, Cell Metab. 11 (4) (2010) 268–272.

[13] T.P. Fitzgibbons, S. Kogan, M. Aouadi, G.M. Hendricks, J. Straubhaar, M.P. Czech, Similarity of mouse perivascular and brown adipose tissues and their resistance to diet-induced inflammation, Am. J. Physiol. Heart Circ. Physiol. 301 (4) (2011) H1425–H1437.
[14] F. Villarroya, R. Cereijo, A. Gavaldà-Navarro, J. Villarroya, M. Giralt, Inflammation of brown/beige adipose tissues in obesity and metabolic disease, J. Intern. Med. 284 (5) (2018) 492–504.
[15] M.A. Mori, T. Thomou, J. Boucher, K.Y. Lee, S. Lallukka, J.K. Kim, M. Torriani, H. Yki-Järvinen, S.K. Grinspoon, A.M. Cypess, C.R. Kahn, Altered miRNA processing disrupts brown/white adipocyte determination and associates with lipodystrophy, J. Clin. Invest. 124 (8) (2014) 3339–3351.
[16] I. Shimizu, K. Walsh, The whitening of brown fat and its implications for weight management in obesity, Curr. Obes. Rep. 4 (2) (2015) 224–229.
[17] C. Vernochet, F. Damilano, A. Mourier, O. Bezy, M.A. Mori, G. Smyth, A. Rosenzweig, N.G. Larsson, C.R. Kahn, Adipose tissue mitochondrial dysfunction triggers a lipodystrophic syndrome with insulin resistance, hepatosteatosis, and cardiovascular complications, FASEB J. 28 (10) (2014) 4408–4419.
[18] Y. Goto, M. Kakizaki, N. Masaki, Production of spontaneous diabetic rats by repetition of selective breeding, Tohoku J. Exp. Med. 119 (1) (1976) 85–90.
[19] A. Kitahara, T. Toyota, M. Kakizaki, Y. Goto, Activities of hepatic enzymes in spontaneous diabetes rats produced by selective breeding of normal Wistar rats, Tohoku J. Exp. Med. 126 (1) (1978) 7–11.
[20] B. Portha, Programmed disorders of beta-cell development and function as one cause for type 2 diabetes? The GK rat paradigm, Diabetes Metab. Res Rev. 21 (6) (2005) 495–504.
[21] W.M.T. Kuwabara, C. Yokota, R. Curi, T.C. Alba-Loureiro, Obesity and type 2 diabetes mellitus induce lipopolysaccharide tolerance in rat neutrophils, Sci. Rep. 8 (1) (2018) 17534.
[22] L.N. Masi, A.R. Martins, J.C. Rosa Neto, C.L. do Amaral, A.R. Crisma, M.A. Vinolo, E.A. de Lima Júnior, S.M. Hirabara, R. Curi, Sunflower oil supplementation has proinflammatory effects and does not reverse insulin resistance in obesity induced by high-fat diet in C57BL/6 mice, J. Biomed. Biotechnol. 2012 (2012), 945131.
[23] E. Bonora, P. Moghetti, C. Zancanaro, M. Cigolini, M. Querena, V. Cacciatori, A. Corgnati, M. Muggeo, Estimates of in vivo insulin action in man: comparison of insulin tolerance tests with euglycemic and hyperglycemic glucose clamp studies, J. Clin. Endocrinol. Metab. 68 (2) (1989) 374–378.
[24] A.C. Panveloski-Costa, S. Silva Teixeira, I.M. Ribeiro, C. Serrano-Nascimento, R. X. das Neves, R.R. Favaro, M. Seelaender, V.R. Antunes, M.T. Nunes, Thyroid hormone reduces inflammatory cytokines improving glycaemia control in alloxan-induced diabetic wistar rats, Acta Physiol. 217 (2) (2016) 130–140.
[25] D.R. Matthews, J.P. Hosker, A.S. Rudenski, B.A. Naylor, D.F. Treacher, R.C. Turner, Homeostasis model assessment: insulin resistance and beta-cell function from fasting plasma glucose and insulin concentrations in man, Diabetologia 28 (7) (1985) 412–419.
[26] A. Katz, S.S. Nambi, K. Mather, A.D. Baron, D.A. Follmann, G. Sullivan, M.J. Quon, Quantitative insulin sensitivity check index: a simple, accurate method for assessing insulin sensitivity in humans, J. Clin. Endocrinol. Metab. 85 (7) (2000) 2402–2410.
[27] H.J. Gundersen, T.F. Bendtsen, L. Korbo, N. Marcussen, A. Møller, K. Nielsen, J. R. Nyengaard, B. Pakkenberg, F.B. Sørensen, A. Vesterby, Some new, simple and efficient stereological methods and their use in pathological research and diagnosis, APMIS 96 (5) (1988) 379–394.
[28] P.M. McKeigue, B. Shah, M.G. Marmot, Relation of central obesity and insulin resistance with high diabetes prevalence and cardiovascular risk in South Asians, Lancet 337 (8738) (1991) 382–386.
[29] L. Chen, D.J. Magliano, P.Z. Zimmet, The worldwide epidemiology of type 2 diabetes mellitus–present and future perspectives, Nat. Rev. Endocrinol. 8 (4) (2011) 228–236.
[30] P.S. Bhatt, W.S. Dhillo, V. Salem, Human brown adipose tissue-function and therapeutic potential in metabolic disease, Curr. Opin. Pharm. 37 (2017) 1–9.
[31] R.K.C. Loh, B.A. Kingwell, A.L. Carey, Human brown adipose tissue as a target for obesity management; beyond cold-induced thermogenesis, Obes. Rev. 18 (11) (2017) 1227–1242.
[32] X.F. Yang, Y.Q. Qiu, L. Wang, K.G. Gao, Z.Y. Jiang, A high-fat diet increases body fat mass and up-regulates expression of genes related to adipogenesis and inflammation in a genetically lean pig, J. Zhejiang Univ. Sci. B 19 (11) (2018) 884–894.
[33] F. Maekawa, K. Fujiwara, D. Kohno, M. Kuramochi, H. Kurita, T. Yada, Young adult-specific hyperphagia in diabetic Goto-kakizaki rats is associated with leptin resistance and elevation of neuropeptide Y mRNA in the arcuate nucleus, J. Neuroendocr. 18 (10) (2006) 748–756.
[34] J.T. Dourmashkin, G.Q. Chang, E.C. Gayles, J.O. Hill, S.K. Fried, C. Julien, S. F. Leibowitz, Different forms of obesity as a function of diet composition, Int J. Obes. 29 (11) (2005) 1368–1378.
[35] P. Trayhurn, R.E. Milner, A commentary on the interpretation of in vitro biochemical measures of brown adipose tissue thermogenesis, Can. J. Physiol. Pharm. 67 (8) (1989) 811–819.
[36] S. Virtue, A. Vidal-Puig, Assessment of brown adipose tissue function, Front Physiol. 4 (2013) 128.
[37] A.W. Fischer, B. Cannon, J. Nedergaard, Leptin: is it thermogenic? Endocr. Rev. 41 (2020) 232–260.
[38] A.S. Divakaruni, D.M. Humphrey, M.D. Brand, Fatty acids change the conformation of uncoupling protein 1 (UCP1), J. Biol. Chem. 287 (44) (2012) 36845–36853.
[39] A. Fedorenko, P.V. Lishko, Y. Kirichok, Mechanism of fatty-acid-dependent UCP1 uncoupling in brown fat mitochondria, Cell 151 (2) (2012) 400–413.
[40] K.O. Doh, Y.W. Kim, S.Y. Park, S.K. Lee, J.S. Park, J.Y. Kim, Interrelation between long-chain fatty acid oxidation rate and carnitine palmitoyltransferase 1 activity with different isoforms in rat tissues, Life Sci. 77 (4) (2005) 435–443.
[41] M. Calderon-Dominguez, J.F. Mir, R. Fucho, M. Weber, D. Serra, L. Herrero, Fatty acid metabolism and the basis of brown adipose tissue function, Adipocyte 5 (2) (2016) 98–118.
[42] Z. Jamal, E.D. Saggerson, Factors influencing the altered thermogenic response of rat brown adipose tissue in streptozotocin-diabetes, Biochem. J. 249 (2) (1988) 415–421.
[43] E. Gonzalez-Hurtado, J. Lee, J. Choi, M.J. Wolfgang, Fatty acid oxidation is required for active and quiescent brown adipose tissue maintenance and thermogenic programing, Mol. Metab. 7 (2018) 45–56.
[44] S.K. Powers, M.P. Wiggs, J.A. Duarte, A.M. Zergeroglu, H.A. Demirel, Mitochondrial signaling contributes to disuse muscle atrophy, Am. J. Physiol. Endocrinol. Metab. 303 (1) (2012) E31–E39.
[45] Y. Alhindi, L.M. Vaanholt, M. Al-Tarrah, S.R. Gray, J.R. Speakman, C. Hambly, B. S. Alanazi, B.M. Gabriel, A. Lionikas, A. Ratkevicius, Low citrate synthase activity is associated with glucose intolerance and lipotoxicity, J. Nutr. Metab. 2019 (2019), 8594825.
[46] A.L. Gasparetti, C.T. de Souza, M. Pereira-da-Silva, R.L. Oliveira, M.J. Saad, E. M. Carneiro, L.A. Velloso, Cold exposure induces tissue-specific modulation of the insulin-signalling pathway in Rattus norvegicus, J. Physiol. 552 (Pt 1) (2003) 149–162.
[47] M. Fasshauer, J. Klein, K. Ueki, K.M. Kriauciunas, M. Benito, M.F. White, C. R. Kahn, Essential role of insulin receptor substrate-2 in insulin stimulation of Glut4 translocation and glucose uptake in brown adipocytes, J. Biol. Chem. 275 (33) (2000) 25494–25501.
[48] K. Rahmouni, D.A. Morgan, G.M. Morgan, X. Liu, C.D. Sigmund, A.L. Mark, W. G. Haynes, Hypothalamic PI3K and MAPK differentially mediate regional sympathetic activation to insulin, J. Clin. Invest. 114 (5) (2004) 652–658.
[49] L.K. Markussen, S. Winther, B. Wicksteed, J.B. Hansen, GSK3 is a negative regulator of the thermogenic program in brown adipocytes, Sci. Rep. 8 (1) (2018) 3469.
[50] J. Nedergaard, T. Bengtsson, B. Cannon, Unexpected evidence for active brown adipose tissue in adult humans, Am. J. Physiol. Endocrinol. Metab. 293 (2) (2007) E444–E452.
[51] J.M. Olsen, M. Sato, O.S. Dallner, A.L. Sandström, D.F. Pisani, J.C. Chambard, E. Z. Amri, D.S. Hutchinson, T. Bengtsson, Glucose uptake in brown fat cells is dependent on mTOR complex 2-promoted GLUT1 translocation, J. Cell Biol. 207 (3) (2014) 365–374.
[52] M. Boutant, M. Joffraud, S.S. Kulkarni, E. García-Casarrubios, P.M. García-Roves, J. Ratajczak, P.J. Fernández-Marcos, A.M. Valverde, M. Serrano, C. Cantó, SIRT1 enhances glucose tolerance by potentiating brown adipose tissue function, Mol. Metab. 4 (2) (2015) 118–131.
[53] G. Navarro, A. Cordomí, V. Casadó-Anguera, E. Moreno, N.S. Cai, A. Cortés, E. I. Canela, C.W. Dessauer, V. Casadó, L. Pardo, C. Lluís, S. Ferré, Evidence for functional pre-coupled complexes of receptor heteromers and adenylyl cyclase, Nat. Commun. 9 (1) (2018) 1242.
[54] C. Cero, H.J. Lea, K.Y. Zhu, F. Shamsi, Y.H. Tseng, A.M. Cypess, β3-Adrenergic receptors regulate human brown/beige adipocyte lipolysis and thermogenesis, JCI Insight 6 (2021) 11.
[55] S. Keipert, M. Jastroch, Brite/beige fat and UCP1 – is it thermogenesis? Biochim Biophys. Acta 1837 (7) (2014) 1075–1082.
[56] A.W. Fischer, J. Behrens, F. Sass, C. Schlein, M. Heine, P. Pertzborn, L. Scheja, J. Heeren, Brown adipose tissue lipoprotein and glucose disposal is not determined by thermogenesis in uncoupling protein 1-deficient mice, J. Lipid Res 61 (11) (2020) 1377–1389.
[57] L. Kazak, E.T. Chouchani, I.G. Stavrovskaya, G.Z. Lu, M.P. Jedrychowski, D. F. Egan, M. Kumari, X. Kong, B.K. Erickson, J. Szpyt, E.D. Rosen, M.P. Murphy, B. S. Kristal, S.P. Gygi, B.M. Spiegelman, UCP1 deficiency causes brown fat respiratory chain depletion and sensitizes mitochondria to calcium overload-induced dysfunction, Proc. Natl. Acad. Sci. USA 114 (30) (2017) 7981–7986.
[58] I.H.N. Luijten, H.M. Feldmann, G. von Essen, B. Cannon, J. Nedergaard, In the absence of UCP1-mediated diet-induced thermogenesis, obesity is augmented even in the obesity-resistant 129S mouse strain, Am. J. Physiol. Endocrinol. Metab. 316 (5) (2019) E729–E740.
[59] P. Oliver, J. Sánchez, A. Caimari, O. Miralles, C. Picó, A. Palou, The intake of a high-fat diet triggers higher brown adipose tissue UCP1 levels in male rats but not in females, Genes Nutr. 2 (1) (2007) 125–126.
[60] T. Fromme, M. Klingenspor, Uncoupling protein 1 expression and high-fat diets, Am. J. Physiol. Regul. Integr. Comp. Physiol. 300 (1) (2011) R1–R8.
[61] E. Hondares, R. Iglesias, A. Giralt, F.J. Gonzalez, M. Giralt, T. Mampel, F. Villarroya, Thermogenic activation induces FGF21 expression and release in brown adipose tissue, J. Biol. Chem. 286 (15) (2011) 12983–12990.
[62] J. Villarroya, R. Cereijo, F. Villarroya, An endocrine role for brown adipose tissue? Am. J. Physiol. Endocrinol. Metab. 305 (5) (2013) E567–E572.
[63] J. Villarroya, R. Cereijo, A. Gavaldà-Navarro, M. Peyrou, M. Giralt, F. Villarroya, New insights into the secretory functions of brown adipose tissue, J. Endocrinol. 243 (2) (2019) R19–R27.
[64] F.M. Fisher, S. Kleiner, N. Douris, E.C. Fox, R.J. Mepani, F. Verdeguer, J. Wu, A. Kharitonenkov, J.S. Flier, E. Maratos-Flier, B.M. Spiegelman, FGF21 regulates PGC-1α and browning of white adipose tissues in adaptive thermogenesis, Genes Dev. 26 (3) (2012) 271–281.
[65] M. Klein Hazebroek, S. Keipert, Adapting to the cold: a role for endogenous fibroblast growth factor 21 in thermoregulation? Front Endocrinol. 11 (2020) 389.

[66] S. Keipert, D. Lutter, B.O. Schroeder, D. Brandt, M. Ståhlman, T. Schwarzmayr, E. Graf, H. Fuchs, M.H. de Angelis, M.H. Tschöp, J. Rozman, M. Jastroch, Author correction: endogenous FGF21-signaling controls paradoxical obesity resistance of UCP1-deficient mice, Nat. Commun. 12 (1) (2021) 1804.
[67] P.G. Cammisotto, M. Bendayan, Leptin secretion by white adipose tissue and gastric mucosa, Histol. Histopathol. 22 (2) (2007) 199–210.
[68] M. Giralt, R. Cereijo, F. Villarroya, Adipokines and the endocrine role of adipose tissues, Handb. Exp. Pharm. 233 (2016) 265–282.
[69] M.J. Hill, S. Kumar, P.G. McTernan, Adipokines and the clinical laboratory: what to measure, when and how? J. Clin. Pathol. 62 (3) (2009) 206–211.
[70] E. Börgeson, C. Godson, Resolution of inflammation: therapeutic potential of pro-resolving lipids in type 2 diabetes mellitus and associated renal complications, Front Immunol. 3 (2012) 318.
[71] C.F. Cheng, H.C. Ku, J.J. Cheng, S.W. Chao, H.F. Li, P.F. Lai, C.C. Chang, M.J. Don, H.H. Chen, H. Lin, Adipocyte browning and resistance to obesity in mice is induced by expression of ATF3, Commun. Biol. 2 (2019) 389.
[72] Y. Zhang, M. Matheny, S. Zolotukhin, N. Tumer, P.J. Scarpace, Regulation of adiponectin and leptin gene expression in white and brown adipose tissues: influence of beta3-adrenergic agonists, retinoic acid, leptin and fasting, Biochim Biophys. Acta 1584 (2002) 115–122.
[73] J.M. Friedman, J.L. Halaas, Leptin and the regulation of body weight in mammals, Nature 395 (6704) (1998) 763–770.
[74] S. Li, H.J. Shin, E.L. Ding, R.M. van Dam, Adiponectin levels and risk of type 2 diabetes: a systematic review and meta-analysis, JAMA 302 (2) (2009) 179–188.
[75] L. Qiao, Hs Yoo, C. Bosco, B. Lee, G.S. Feng, J. Schaack, N.W. Chi, J. Shao, Adiponectin reduces thermogenesis by inhibiting brown adipose tissue activation in mice, Diabetologia 57 (5) (2014) 1027–1036.
[76] C.M. Steppan, S.T. Bailey, S. Bhat, E.J. Brown, R.R. Banerjee, C.M. Wright, H. R. Patel, R.S. Ahima, M.A. Lazar, The hormone resistin links obesity to diabetes, Nature 409 (6818) (2001) 307–312.
[77] É. Szentirmai, L. Kapás, The role of the brown adipose tissue in β3-adrenergic receptor activation-induced sleep, metabolic and feeding responses, Sci. Rep. 7 (1) (2017) 958.
[78] H. Kim, P.A. Pennisi, O. Gavrilova, S. Pack, W. Jou, J. Setser-Portas, J. East-Palmer, Y. Tang, V.C. Manganiello, D. Leroith, Effect of adipocyte beta3-adrenergic receptor activation on the type 2 diabetic MKR mice, Am. J. Physiol. Endocrinol. Metab. 290 (6) (2006) E1227–E1236.
[79] K.B. Ohlson, N. Mohell, B. Cannon, S.G. Lindahl, J. Nedergaard, Thermogenesis in brown adipocytes is inhibited by volatile anesthetic agents. A factor contributing to hypothermia in infants? Anesthesiology 81 (1) (1994) 176–183.
[80] K.B. Ohlson, I.G. Shabalina, K. Lennström, E.C. Backlund, N. Mohell, G. E. Bronnikov, S.G. Lindahl, B. Cannon, J. Nedergaard, Inhibitory effects of halothane on the thermogenic pathway in brown adipocytes: localization to adenylyl cyclase and mitochondrial fatty acid oxidation, Biochem. Pharm. 68 (3) (2004) 463–477.
[81] J.M. Olsen, R.I. Csikasz, N. Dehvari, L. Lu, A. Sandström, A.I. Öberg, J. Nedergaard, S. Stone-Elander, T. Bengtsson, β3-Adrenergically induced glucose uptake in brown adipose tissue is independent of UCP1 presence or activity: mediation through the mTOR pathway, Mol. Metab. 6 (6) (2017) 611–619.
[82] M. Rosenbaum, R.L. Leibel, Adaptive thermogenesis in humans, Int J. Obes. 34 (Suppl 1) (2010) S47–S55.
[83] C. Lapa, P. Arias-Loza, N. Hayakawa, H. Wakabayashi, R.A. Werner, X. Chen, T. Shinaji, K. Herrmann, T. Pelzer, T. Higuchi, Whitening and impaired glucose utilization of brown adipose tissue in a rat model of type 2 diabetes mellitus, Sci. Rep. 7 (1) (2017) 16795.
[84] S. Rodovalho, B. Rachid, J.C. De-Lima-Junior, S. van de Sande-Lee, J. Morari, H. M. Carvalho, B.J. Amorim, A.J. Tincani, E. Chaim, J.C. Pareja, M.J. Saad, F. Folli, C.D. Ramos, B. Geloneze, L.A. Velloso, Impairment of body mass reduction-associated activation of brown/beige adipose tissue in patients with type 2 diabetes mellitus, Int J. Obes. 41 (11) (2017) 1662–1668.
[85] M.V. Wu, G. Bikopoulos, S. Hung, R.B. Ceddia, Thermogenic capacity is antagonistically regulated in classical brown and white subcutaneous fat depots by high fat diet and endurance training in rats: impact on whole-body energy expenditure, J. Biol. Chem. 289 (49) (2014) 34129–34140.
[86] E.S. Bachman, H. Dhillon, C.Y. Zhang, S. Cinti, A.C. Bianco, B.K. Kobilka, B. B. Lowell, betaAR signaling required for diet-induced thermogenesis and obesity resistance, Science 297 (5582) (2002) 843–845.
[87] Y. Nishimoto, Y. Tamori, CIDE family-mediated unique lipid droplet morphology in white adipose tissue and brown adipose tissue determines the adipocyte energy metabolism, J. Atheroscler. Thromb. 24 (10) (2017) 989–998.
[88] S. Enerbäck, A. Jacobsson, E.M. Simpson, C. Guerra, H. Yamashita, M.E. Harper, L. P. Kozak, Mice lacking mitochondrial uncoupling protein are cold-sensitive but not obese, Nature 387 (6628) (1997) 90–94.
[89] A.W. Fischer, C.S. Hoefig, G. Abreu-Vieira, J. de Jong, N. Petrovic, J. Mittag, B. Cannon, J. Nedergaard, Leptin raises defended body temperature without activating thermogenesis, Cell Rep. 14 (7) (2016) 1621–1631.

Update

Biomedicine & Pharmacotherapy

Volume 146, Issue , February 2022, Page

DOI: https://doi.org/10.1016/j.biopha.2021.112612

Biomedicine & Pharmacotherapy 146 (2022) 112612

Contents lists available at ScienceDirect

Biomedicine & Pharmacotherapy

journal homepage: www.elsevier.com/locate/biopha

Corrigendum

Corrigendum to "Impaired brown adipose tissue is differentially modulated in insulin-resistant obese wistar and type 2 diabetic Goto-Kakizaki rats" [Biomed. Pharmacother. 142 (2021) 112019]

Tamires Duarte Afonso Serdan [a,*], Laureane Nunes Mais [a], Joice Naiara Bertaglia Pereira [a], Luiz Eduardo Rodrigues [a], Amanda Lins Alecrim [a], Maria Vitoria Martins Scervino [a], Vinicius Leonardo Sousa Diniz [a], Alef Aragão Carneiro dos Santos [a], Celso Pereira Batista Sousa Filho [a], Tatiana Carolina Alba-Loureiro [a], Gabriel Nasri Marzuca-Nassr [b], Roberto Barbosa Bazotte [c], Renata Gorjão [a], Tania Cristina Pithon-Curi [a], Rui Curi [a], Sandro Massao Hirabara [a]

[a] Interdisciplinary Postgraduate Program in Health Sciences, Cruzeiro do Sul University, São Paulo, Brazil
[b] Department of Inner Medicine and Master in Physical Therapy, Faculty of Medicine, Universidad de La Frontera, Temuco, Chile
[c] Department of Pharmacology and Therapeutics, State University of Maringa, Paraná, Brazil

The authors regret that there are some errors in the description of the "2.10 Positron emission tomography with 2-deoxy-2-[fluorine-18]fluoro-D-glucose (^{18}F-FDG PET)" section. The results and analysis of the our data remain correct and unchanged. The correct description of the 2.10 section is detailed as follow:

"To evaluate BAT activity, ^{18}F-FDG PET images were acquired at 14 weeks of age using a small-animal PET Scanner (Triumph™ – Gamma Medica-Ideas, Northridge, CA, U.S.A). Briefly, animals were housed 24 h before PET scans at the facility of Nuclear Medicine Laboratory (LIM-43), University of São Paulo, São Paulo, Brazil. The bolus of 37–55 MBq of ^{18}F-FDG was administered in the penile vein under adrenergic stimulation or basal conditions. Under stimulated conditions, an intravenous injection of CL316,243 (1 mg/kg) was given 30 min before ^{18}F-FDG administration. In the basal state, animals received an intravenous saline injection. Images were acquired 45 min after ^{18}F-FDG injection, with the animal under isoflurane inhalation anesthesia (1.5–3%).

Emission sinograms were iteratively reconstructed with the algorithm OSEM 3D; 20 iterations and 4 subsets, after being normalized and corrected for scatter and radioactivity decay. Polygonal regions of interest were drawn on sagittal PET slices for interscapular BAT. Circular regions of interest were placed in the left lung as background activity. From each region of interest, mean standardized uptake values (SUVs mean) and target-to-background ratios were measured as indices of ^{18}F-FDG uptake.

PhD. Caroline Cristiano Real Gregório and PhD. Daniele de Paula Faria, from the Laboratory of Nuclear Medicine of the University of Sao Paulo (LIM-43), Sao Paulo, Brazil, revised the description of the methodology for PET-CT protocol, performed the experiments related to this protocol, and helped with the data interpretation and presentation of the results from Fig. 10".

The authors would like to apologise for any inconvenience caused.

DOI of original article: https://doi.org/10.1016/j.biopha.2021.112019.
* Correspondence to: Interdisciplinary Postgraduate Program in Health Sciences, Cruzeiro do Sul University, Rua Galvao Bueno, 868, Liberdade, São Paulo, SP 01506-000, Brazil.
E-mail address: tamiresd.serdan@gmail.com (T.D.A. Serdan).

https://doi.org/10.1016/j.biopha.2021.112612

Available online 6 January 2022